

Symmetry analysis of current-induced switching of antiferromagnets

Hikaru Watanabe* and Youichi Yanase

Department of Physics, Graduate School of Science, Kyoto University, Kyoto 606-8502, Japan

(Dated: January 1, 2019)

Antiferromagnets are robust to external electric and magnetic fields, and hence are seemingly uncontrollable. Recent studies, however, realized the electrical manipulations of antiferromagnets by virtue of the antiferromagnetic Edelstein effect. We present a general symmetry analysis of electrically switchable antiferromagnets based on group-theoretical approaches. Furthermore, we identify a direct relation between switchable antiferromagnets and the ferrotoroidic order. The concept of the ferrotoroidic order clarifies the unidirectional nature of switchable antiferromagnets and provides a criterion for the controllability of antiferromagnets. The scheme paves a way for perfect writing and reading of switchable antiferromagnets.

The spin degree of freedom is highly controllable and has opened a new paradigm of electronics [1–4]. Especially, spin manipulation by an interplay with other degrees of freedom such as charge and valley is attracting much interest in the field of spintronics. The concept is widespread in condensed matter physics, *e.g.*, superconductors [5] and topological materials [6].

Recently, the possibility of manipulating antiferromagnets has been recognized [7–11], while most spintronics devices are based on ferromagnets. The antiferromagnet, which in itself has neither electric nor magnetic polarizations, is robust to external electric and magnetic fields, in contrast to ferroelectric or ferromagnetic material-based devices. Hence, antiferromagnets are considered to be a new candidate for a nonvolatile memory device [12].

The switching of antiferromagnets has been explored in various ways: by using a spin-transfer torque or spin current in heterostructures [13–15] or magnetoelectric effects in bulk antiferromagnets [16]. In particular, manipulation by an electric current has significantly promoted the controllability of antiferromagnets. The switching mechanism utilizes current-induced antiferroic magnetization, namely, the antiferromagnetic (AFM) Edelstein effect. Following a theoretical proposal submitted independently by some groups [17, 18], experimental realizations of switching have been achieved in CuMnAs [12] and Mn₂Au [19].

The key to the AFM Edelstein effect is a *locally* non-centrosymmetric crystalline structure, in which the local symmetry of certain sites has no parity symmetry in spite of a globally centrosymmetric crystalline symmetry. The sublattice degree of freedom plays an important role in such systems. The parity symmetry is preserved since the atoms in each sublattice are interchanged by the parity operation. Then, spin-momentum locking arises in a sublattice-dependent manner although uniform spin-momentum locking is forbidden due to the globally centrosymmetric crystal symmetry [20–24]. Accordingly, nonequilibrium *antiferroic* spin polarization is induced under electric current. This is an analog to the Edelstein effect, that is, current-induced ferroic spin polarization [25–28].

The switchable AFM order, which shares the same symmetry with current-induced antiferroic magnetization, breaks both of inversion and time-reversal symmetry although it preserves translational symmetry. It is noteworthy that the combined symmetry of parity and time-reversal operations, namely, \mathcal{PT} symmetry, is preserved. The \mathcal{PT} symmetry forbids electric polarization and net magnetization and ensures invulnerability to external electric or magnetic fields.

The properties of the AFM Edelstein effect have been investigated in previous studies [17, 18, 29–31]. The general criterion for determining electrically switchable antiferromagnets, however, remains unclear. An incomplete understanding of switchable antiferromagnets has disrupted further explorations of candidate materials except for the existing candidates [12, 19].

In our work, we present a general criterion for the current-induced switching of antiferromagnets. A symmetry analysis based on the magnetic representation theory and the Aizu species clarifies what kind of AFM order can be manipulated by the AFM Edelstein effect. Furthermore, the analysis links switchable antiferromagnets and ferrotoroidic order. Thus, this work not only identifies many candidate materials but also provides a clear viewpoint of AFM spintronics. In the following, we do not discuss the effect of spin-transfer torque and spin current, since we focus on bulk antiferromagnets which are insensitive to surfaces.

Representation analysis. We first present a symmetry analysis of magnetic modes induced by the AFM Edelstein effect. The analysis is carried out with the use of a magnetic representation theory [32–35]. We focus on centrosymmetric systems where the \mathcal{PT} symmetry is preserved, though it is straightforward to extend the analysis to noncentrosymmetric systems. Noncentrosymmetric magnets (Ga,Mn)As and MnSiN₂ are exemplified in Supplemental Material [35].

The magnetic modes realized by the AFM Edelstein effect do not lead to any translational symmetry breaking, and hence they are characterized by the Néel vector $\mathbf{Q} = \mathbf{0}$. The formula of the AFM Edelstein effect is writ-

ten as

$$\hat{m}^{\text{AF}} = \hat{\kappa} \mathbf{j}, \quad (1)$$

where the susceptibility tensor $\hat{\kappa}$ has symmetry determined by the crystalline structure [22, 30]. Therefore, supposing systems in the paramagnetic phase, we here identify the AFM mode \hat{m}^{AF} and investigate which components of $\hat{\kappa}$ are allowed.

The allowed magnetic symmetry with $\mathbf{Q} = \mathbf{0}$ is described by a magnetic representation

$$\Gamma_{\mathbf{G}}^{\text{mag}}(\mathbf{H}) = \Gamma_{\mathbf{G}}^{\text{P}}(\mathbf{H}) \otimes \Gamma_{\mathbf{G}}^{\text{M}}, \quad (2)$$

where \mathbf{G} and \mathbf{H} denote a crystal group and site-symmetry group of magnetic sites, respectively. $\Gamma_{\mathbf{G}}^{\text{P}}$ is a permutation representation of magnetic sites and $\Gamma_{\mathbf{G}}^{\text{M}}$ is a representation of an axial vector. The basis \hat{m}^{AF} of allowed magnetic modes is explicitly denoted as $m_{\mu}^{(\tau)}$, where τ and μ are indices of the basis of $\Gamma_{\mathbf{G}}^{\text{P}}$ and $\Gamma_{\mathbf{G}}^{\text{M}}$, respectively.

The response formula (1) is explicitly recast

$$m_{\mu}^{(\tau)} = \kappa_{\tau\mu;\nu} j_{\nu}. \quad (3)$$

The coefficient $\kappa_{\tau\mu;\nu}$ is transformed by a symmetry operation $g \in \mathbf{G}$ as [39]

$$g(\kappa_{\tau\mu;\nu}) = \sum_{\rho,\lambda,\kappa} \kappa_{\rho\lambda;\kappa} [D^{(\text{P})}(g)]_{\rho\tau} [D^{(\text{M})}(g)]_{\lambda\mu} [D^{(\text{j})}(g)]_{\kappa\nu}, \quad (4)$$

where $D^{(\text{P})}$, $D^{(\text{M})}$, and $D^{(\text{j})}$ are representation matrices of the sublattice permutation, axial vector, and polar vector, respectively. According to Neumann's principle, the transformed susceptibility tensor should satisfy $g(\hat{\kappa}) = \hat{\kappa}$ [40, 41]. Thus, the susceptibility tensor $\hat{\kappa}$ is subject to constraints from the crystal group \mathbf{G} .

An algebraic calculation by Eq. (4) identifies the symmetry-adapted form of $\kappa_{\tau\mu;\nu}$. To examine the symmetry constraints between magnetic structures and electric currents, it is practical to decompose the representation of the susceptibility tensor $\kappa_{\tau\mu;\nu}$ into irreducible representations of \mathbf{G} , that is, $\{\Gamma_{\mathbf{G}}^{(\alpha)}\}$. The decomposition is obtained as

$$\Gamma_{\mathbf{G}}^{\text{mag}}(\mathbf{H}) \otimes \Gamma_{\mathbf{G}}^{\text{j}} = \sum_{\alpha} q_{\alpha} \Gamma_{\mathbf{G}}^{(\alpha)}, \quad (5)$$

where a coefficient q_{α} denotes a frequency of $\Gamma_{\mathbf{G}}^{(\alpha)}$ in the summation. $\Gamma_{\mathbf{G}}^{\text{j}}$ is a representation of the polar vector. The coefficient q_1 for the identity representation $\Gamma_{\mathbf{G}}^{(1)}$ gives the number of independent components of $\hat{\kappa}$.

Here, we summarize the symmetry constraints for switchable antiferromagnets. Each irreducible representation $\Gamma_{\mathbf{G}}^{(\alpha)}$ has inversion parity, since the crystal group \mathbf{G} is centrosymmetric. Although both $\Gamma_{\mathbf{G}}^{\text{M}}$ and $\Gamma_{\mathbf{G}}^{\text{j}}$ are representations of vector quantities, they have opposite

parity. Thus, the permutation representation $\Gamma_{\mathbf{G}}^{\text{P}}$ should comprise odd-parity irreducible representations to satisfy $q_1 \neq 0$. This means that a locally noncentrosymmetric property of magnetic sites is required for the AFM Edelstein effect as mentioned in previous studies [17, 18, 30]. Furthermore, the magnetic representation $\Gamma_{\mathbf{G}}^{\text{mag}}$ should comprise a polar representation $\Gamma_{\mathbf{G}}^{\text{j}}$. Owing to the time-reversal even/odd (\mathcal{T} even/ \mathcal{T} odd) nature of the representation $\Gamma_{\mathbf{G}}^{\text{P}}/\Gamma_{\mathbf{G}}^{\text{M}}$, the magnetic mode $m_{\mu}^{(\tau)}$ is \mathcal{T} odd and leads to the time-reversal symmetry breaking.

From the above analysis we conclude that the current-induced magnetic structure is polar and magnetic (\mathcal{T} odd). It follows that the switchable AFM order by the AFM Edelstein effect contains a *toroidal moment* \mathbf{T} [42]. We stress that the Néel vector is $\mathbf{Q} = \mathbf{0}$. Thus, all the switchable AFM order is regarded as a ferroic toroidal order, namely, ferrotoroidic order. This is a criterion of materials for AFM spintronics.

The toroidic nature of switchable antiferromagnets is intuitively understood by the fact that the electric current gives rise to a shift of the Fermi surface and produces ‘‘polarization’’ in momentum space. Such polarization shares the same symmetry with the toroidal moment as we have shown in the group-theoretical classification [43].

Aizu species. Regarding the switchable AFM order as ferrotoroidic order, we may clarify the possibility of AFM domain switching by making use of the *Aizu species*.

In general, a phase transition reduces the symmetry operations of a disordered phase. The symmetry relation between the disordered and ordered phases is formulated by a group-theoretical method. By supposing the crystal group $\mathbf{G}(\mathbf{K})$ in the disordered (ordered) phase, the coset decomposition of \mathbf{G} by \mathbf{K} is obtained as

$$\mathbf{G} = g_1\mathbf{K} + g_2\mathbf{K} + \cdots + g_N\mathbf{K}, \quad (6)$$

where $g_1 \in \mathbf{K}$ and $g_j \notin \mathbf{K}$ ($j \neq 1$). N is the order of \mathbf{G} divided by that of \mathbf{K} . A domain state s_1 , which is invariant to the symmetry operations of \mathbf{K} , is transformed into other domain states by symmetry operations of $g_j\mathbf{K}$ ($j \neq 1$). Therefore, the coset decomposition (6) shows the relation between domain states $\{s_j\}$,

$$s_j = g_j g_i^{-1} s_i, \quad (7)$$

where the domain s_j is invariant to the symmetry operations of $\mathbf{K}_j = g_j\mathbf{K}g_j^{-1}$.

Domain properties of the ordered phase are classified by the Aizu species [44–50], the ensemble of pairs of \mathbf{G} and \mathbf{K} written as \mathbf{GFK} . In the Aizu species classification, the species \mathbf{GFK} is characterized by physical quantities such as electric polarization, magnetization, strain, and toroidal moment. In the case of ferrotoroidic order, we first assign a domain s_1 with a toroidal moment $\mathbf{T}^{(1)}$. Correspondingly, we obtain the toroidal moment

$$\mathbf{T}^{(j)} = g_j \mathbf{T}^{(1)} \quad (8)$$

for another domain s_j . The number of possible toroidal moments is determined by a given species, since the species \mathbf{GFK} imposes the algebraic relation between domains as Eq. (7). Therefore, the Aizu species \mathbf{GFK} is classified as full/partial/zero toroidic, when the domain states are completely/partially/not distinguishable by the toroidal moment \mathbf{T} . The classification is summarized in Table I.

TABLE I. The classification of Aizu species \mathbf{GFK} based on toroidal moments $\{\mathbf{T}^{(i)}\}$.

$\{\mathbf{T}^{(i)}\}$	\mathbf{GFK}
$\mathbf{T}^{(i)} \neq \mathbf{T}^{(j)}$ for all i, j	full toroidic
$\mathbf{T}^{(i)} = \mathbf{T}^{(j)}$ for some but not all i, j	partial toroidic
$\mathbf{T}^{(i)} = \mathbf{T}^{(j)} = 0$ for all i, j	zero toroidic

In a full- or partial toroidic species, the symmetry-adapted field for the toroidal moment \mathbf{T} , that is, electric current \mathbf{j} , energetically distinguishes the domain states completely or partially. The electric current acts on the AFM moment such that the toroidal moment arising from the AFM mode is aligned along the injected current. Therefore, the classification based on the Aizu species for the ferrotoroidic order clarifies the AFM domains which are controllable by the electric current \mathbf{j} . With a pair of the crystal group \mathbf{G} and the group for the AFM state \mathbf{K} , the feasibility of the electrical switching of AFM domains is determined by referring to the toroidic property of the Aizu species [49].

The switchable antiferromagnets should belong to the full- or partial toroidic species. We have identified candidate materials for the switchable AFM order and show a part of the list in Table II. In Supplemental Material, we can find more candidates and more detailed information [35]. In the following, we apply our symmetry analysis to some antiferromagnets and reveal the toroidic property of the AFM state.

Similarly,

Full toroidic case. As an example of the ferrotoroidic case, we discuss the tetragonal CuMnAs [61] where AFM domain switching has been demonstrated [12]. The crystal group is $4/mmm$ which is represented as $\mathbf{G} = 4/mmm1'$ in magnetic point group notation. The AFM phase is specified by $\mathbf{K} = mmm'\langle x \rangle$, where the symbol $\langle x \rangle$ means the twofold rotation symmetry along the x axis. Correspondingly, the Aizu species is denoted by

$$4/mmm1' Fmmm'\langle x \rangle. \quad (9)$$

The coset decomposition (6) is obtained as

$$\mathbf{G} = I\mathbf{K} + P\mathbf{K} + C_{4z}^+\mathbf{K} + S_{4z}^+\mathbf{K}, \quad (10)$$

where I , P , and C_{4z}^+ (S_{4z}^+) are the identity operation, the parity operation, and the four-fold (improper) rotation,

TABLE II. List of candidate materials. The table lists metallic or semiconducting compounds, crystal point group (PG), direction of toroidal moment (\mathbf{T}), Néel temperatures (T_N), and references (Ref.). More candidates are shown in Supplemental Material [35].

Compounds	PG	\mathbf{T}	T_N	Ref.
PrMnSbO	$4/mmm$		$35 < T < 230$	[51]
		$\{T_x, T_y\}$	35	[51]
NdMnAsO	$4/mmm$		$23 < T < 359$	[52, 53]
		$\{T_x, T_y\}$	23	[52, 53]
DyB ₄	$4/mmm$	$\{T_x, T_y\}$	$12.7 < T < 20.3$	[54–56]
ErB ₄	$4/mmm$	$\{T_x, T_y\}$	13	[54, 55, 57]
Mn ₂ Au	$4/mmm$	$\{T_x, T_y\}$	> 1000	[58]
FeSn ₂	$4/mmm$	$\{T_x, T_y\}$	$93 < T \lesssim 378$	[59, 60]
		$\{T_x, T_y\}$	$93 \lesssim T < 378$	[59, 60]
CuMnAs	$4/mmm$	$\{T_x, T_y\}$	480	[61]
U ₃ Ru ₄ Al ₁₂	$6/mmm$	T_z	9.5	[62, 63]
CaMn ₂ Bi ₂	$\bar{3}m$	$\{T_x, T_y\}$	154	[64]
SrMn ₂ Sb ₂	$\bar{3}m$	$\{T_x, T_y\}$	110	[65]
Gd ₅ Ge ₄	mmm	T_z	127	[66, 67]
UCu ₅ In	mmm	T_y	25	[68]
YbAl _{1-x} Fe _x B ₄	mmm	T_x		[69]

respectively. The domain s_1 with the polar axis x possesses the toroidal moment $\mathbf{T}^{(1)} = T\hat{x}$. Accordingly, the toroidal moment of the domain $s_2 = Ps_1$ is obtained as

$$\mathbf{T}^{(2)} = P(T\hat{x}) = -T\hat{x}. \quad (11)$$

Similarly, $\mathbf{T}^{(3)} = T\hat{y}$ and $\mathbf{T}^{(4)} = -T\hat{y}$ are obtained for the domains s_3 and s_4 , respectively. Thus, all the domains of CuMnAs have different toroidal moments, and the Aizu species (9) is actually full toroidic. Therefore, the AFM state can be completely manipulated by the electric current.

We summarize the properties of the Aizu species in Eq. (9) in Table III. The species (9) is zero electric and zero magnetic, and hence AFM domains can hold neither electric polarization \mathbf{P} nor magnetic polarization \mathbf{M} . These constraints are consistent with the \mathcal{PT} symmetry preserved in the AFM state. On the other hand, the species is partial elastic. It follows that the AFM domains are partially controllable by stress which is the conjugate field to the strain $\hat{\epsilon}$. Thus, the Aizu species analysis is also useful to elucidate the possibility of an indirect switching of the AFM state.

TABLE III. The characterization of the Aizu species of CuMnAs [49]. “F,” “P,” and “Z” represent full, partial, and zero, respectively.

$4/mmm1' Fmmm'\langle x \rangle$	$\hat{\epsilon}$	\mathbf{P}	\mathbf{M}	\mathbf{T}
	P	Z	Z	F

To support the Aizu species analysis, we conduct a

representation analysis. The magnetic Mn ions are positioned in the crystallographic site with a noncentrosymmetric site-symmetry group $\mathbf{H} = 4mm$, and CuMnAs is locally noncentrosymmetric. The magnetic representation is obtained as

$$\Gamma_{\mathbf{G}}^{\text{mag}}(\mathbf{H}) = \Gamma_{\mathbf{G}}^{\text{P}}(\mathbf{H}) \otimes \Gamma_{\mathbf{G}}^{\text{M}}, \quad (12)$$

$$= A_{2g} + E_g + A_{1u} + E_u. \quad (13)$$

Then, the product representation (5) comprises $\Gamma_{\mathbf{G}}^{(1)} = A_{1g}$, since the E_u mode in Eq. (13) is included in the polar representation $\Gamma_{\mathbf{G}}^j = A_{2u} + E_u$. Thus, the AFM Edelstein effect is allowed. The correspondence between the toroidal moment and the AFM order is clarified by the projection operator method [32, 35]. By the projection operator associated with the basis of E_u , the AFM moment aligned along the $\pm x$ axis is revealed to have a toroidal moment $\pm T\hat{y}$. Hence, the in-plane electric current $\pm j_y$ stabilizes the AFM state as shown in Fig 1. Similarly, the electric current $\pm j_x$ stabilizes the AFM moment along the $\pm y$ axis which has the toroidal moment $\pm T\hat{x}$. Thus, the representation theory is consistent with the Aizu species analysis.

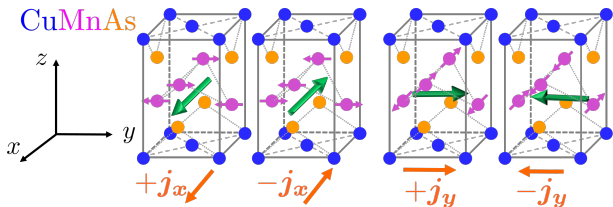


FIG. 1. The correspondence between the AFM domain and the toroidal moment in CuMnAs. The green (purple) colored arrows represent the toroidal (magnetic) moments. The electric current stabilizing each domain is depicted.

Partial toroidic case. Next, we discuss a partially controllable AFM state of $\text{U}_3\text{Ru}_4\text{Al}_{12}$, which belongs to a partial toroidic species.

$\text{U}_3\text{Ru}_4\text{Al}_{12}$ crystallizes in a hexagonal structure ($\mathbf{G} = 6/mmm$). The magnetic uranium ions form a kagomé lattice [62, 63]. Interestingly, the compound shows a compensated and noncollinear AFM order by which the threefold rotation symmetries are broken [63]. The Aizu species is given by

$$6/mmm1' Fmmm' \langle z \rangle, \quad (14)$$

where $\langle z \rangle$ means the twofold rotation symmetry along the z axis. The species is partial toroidic as shown in Table IV and allows the domain states to be partially controllable by the electric current. Following the algebraic relation between the domain states, half of the six domains host the same toroidal moment $\mathbf{T} \parallel \hat{z}$ which can be inverted by the out-of-plane electric current j_z .

We also present a representation analysis. The U atoms are positioned in crystallographic sites with the

TABLE IV. The characterization of the Aizu species of $\text{U}_3\text{Ru}_4\text{Al}_{12}$ [49].

$6/mmm1' Fmmm' \langle z \rangle$	\hat{e}	\mathbf{P}	\mathbf{M}	\mathbf{T}
	P	Z	Z	P

site-symmetry group $\mathbf{H} = mm2$. The magnetic representation is obtained as

$$\Gamma_{\mathbf{G}}^{\text{mag}}(\mathbf{H}) = A_{2g} + B_{1g} + B_{2g} + A_{1u} + A_{2u} + B_{1u} + 2E_{1g} + E_{2g} + E_{1u} + 2E_{2u}, \quad (15)$$

which comprises polar representations A_{2u} and E_{1u} . The basis of A_{2u} (E_{1u}) can be taken as a toroidal moment $\mathbf{T} \parallel \hat{z}$ ($\mathbf{T} \parallel \{\hat{x}, \hat{y}\}$), and the AFM Edelstein effect is actually allowed when $\mathbf{j} \parallel \hat{z}$ ($\mathbf{j} \parallel \{\hat{x}, \hat{y}\}$).

The magnetic order of $\text{U}_3\text{Ru}_4\text{Al}_{12}$ [63] is represented by the A_{2u} and E_{2u} irreducible representations. These representations are odd parity, and the former (latter) is polar (nonpolar). By representing one of the magnetic domains by the basis $\phi_{E_{2u}} + \phi_{A_{2u}}$, the other AFM domains are labeled as depicted in Fig 2. The $\phi_{A_{2u}}$ mode corresponds to the toroidal moment T_z , and hence the electric current j_z enables the switching between the AFM domains having different $\phi_{A_{2u}}$ components. On the other hand, the domains with the same $\phi_{A_{2u}}$ components cannot be switched by the electric current. Thus, the representation analysis is consistent with the Aizu species analysis in a partial toroidic case of $\text{U}_3\text{Ru}_4\text{Al}_{12}$. To control the AFM domains perfectly, we may use the magnetopiezoelectric effect, which is explained in Supplemental Material [35].

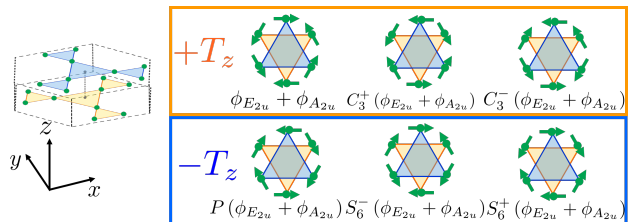


FIG. 2. The Uranium sites in $\text{U}_3\text{Ru}_4\text{Al}_{12}$ (left) and the possible AFM domains (right panels) [63]. C_3^\pm (S_6^\pm) denotes the three-fold (improper) rotation. Each of domains has a toroidal moment, $\pm T\hat{z}$.

Read-out of AFM domains. Following the symmetry analysis revealing an essential role of ferrotoroidic order for the electrical switching of AFM domains, we present a complete read-out of the domains using a functionality arising from the unidirectional nature of the ferrotoroidic order.

In an experiment of CuMnAs, an electrical read-out of AFM domains has been performed by measuring anisotropic magnetoresistance (AMR) [12]. The AMR, however, cannot completely distinguish domains, because

domains with opposite toroidal moments show the same AMR. On the other hand, we can make use of the *uni-directional* property of the ferrotoroidic order to discern the AFM domains in a complete way.

The ferrotoroidic order induces a unidirectional anisotropy in various transport phenomena: In a nonlinear electric conductivity up to the second order $|\mathbf{E}|^2$ denoted by

$$\mathbf{j}_\mu = \sigma_{\mu\nu} E_\nu + \tilde{\sigma}_{\mu\nu} E_\nu^2, \quad (16)$$

the ferrotoroidic moment $\mathbf{T} \parallel \hat{x}_\mu$ gives rise to a finite longitudinal component $\tilde{\sigma}_{\mu\mu}$, which changes sign between domains with opposite toroidal moment [43]. Therefore, the nonlinear conductivity may distinguish the domain states of switchable antiferromagnets in a complete manner. Thus, both of the manipulation and detection of AFM states can be electrically carried out.

The nonlinear conductivity $\tilde{\sigma}_{\mu\mu}$ indicates a dichromatic transport. Indeed, dichromatic transport is an emergent physical property induced by the ferrotoroidic order. Although dichromatic transport has been observed in noncentrosymmetric systems under an external magnetic field [70–73] and several ferromagnetic materials [74, 75], it may be realized in ferrotoroidic AFM states without a magnetic field. Such dichroism induced by the ferrotoroidic order is tunable by the current \mathbf{j} through AFM domain switching. When we vary an electric current, a hysteretic behavior may be observed as a signal of AFM domain switching.

It is noteworthy that the manipulation and detection of the ferrotoroidic domain by a tunable electric current are realizable only in metallic systems in contrast to previous observations of ferrotoroidic order in magnetic insulators [42, 76, 77]. The toroidic domain in insulators can be manipulated by making use of the magnetoelectric effect. To be specific, the toroidic domain in insulators is inverted by simultaneously applying both electric and magnetic fields [76, 77]. In contrast, the toroidic domains in metals are controllable by only injecting the electric current.

To summarize, we provide a general criterion of electrically switchable antiferromagnets based on the complementary use of the Aizu species and the representation theory. Both approaches unveil the direct correspondence between switchable AFM states and ferrotoroidic order. The concept of ferrotoroidic order uncovers functionalities of antiferromagnets and gives a clear viewpoint in AFM spintronics. It is desirable for further developments of AFM spintronics to explore the functionalities of various antiferromagnets. On the basis of the symmetry analysis, we provided a list of electrically switchable antiferromagnets, which will be useful for future studies.

Recently, we became aware of an experiment of CuMnAs which demonstrated the switching and reading of the AFM domain states with opposite toroidal moments [78].

The domain states have been distinguished by the nonlinear Hall conductivity which is described by Eq. (16). The toroidal moment $\mathbf{T} \parallel \hat{x}_\mu$ gives rise to a transverse nonlinear conductivity $\tilde{\sigma}_{\mu\nu}$ [79], and hence the experimental result [78] is consistent with our symmetry analysis.

Acknowledgments— The authors are grateful to M. Kimata, S. Nakatsuji, and S. Suzuki for fruitful discussions. This work is supported by a Grant-in-Aid for Scientific Research on Innovative Areas “J-Physics” (Grant No. JP15H05884) and “Topological Materials Science” (Grant No. JP16H00991, JP18H04225) from the Japan Society for the Promotion of Science (JSPS), and by JSPS KAKENHI (Grants No. JP15K05164, No. JP15H05745, and No. JP18H01178). H.W. is supported by a JSPS research fellowship and supported by JSPS KAKENHI (Grant No. 18J23115).

* watanabe.hikaru.43n@st.kyoto-u.ac.jp

- [1] I. Žutić, J. Fabian, and S. D. Sarma, *Rev. Mod. Phys.* **76**, 323 (2004).
- [2] Y. Tserkovnyak, A. Brataas, G. E. W. Bauer, and B. I. Halperin, *Rev. Mod. Phys.* **77**, 1375 (2005).
- [3] C. Chappert, A. Fert, and F. N. Van Dau, *Nat. Mater.* **6**, 813 (2007).
- [4] A. D. Kent and D. C. Worledge, *Nat. Nanotechnol.* **10**, 187 (2015).
- [5] J. Linder and J. W. A. Robinson, *Nat. Phys.* **11**, 307 (2015).
- [6] Y. Shiomi, K. Nomura, Y. Kajiwara, K. Eto, M. Novak, K. Segawa, Y. Ando, and E. Saitoh, *Phys. Rev. Lett.* **113**, 196601 (2014).
- [7] A. H. MacDonald and M. Tsoi, *Philos. Trans.: Math., Phys. Eng. Sci.* **369**, 3098 (2011).
- [8] E. V. Gomonay and V. M. Loktev, *Low Temp. Phys.* **40**, 17 (2014).
- [9] T. Jungwirth, X. Marti, P. Wadley, and J. Wunderlich, *Nat. Nanotechnol.* **11**, 231 (2016).
- [10] V. Baltz, A. Manchon, M. Tsoi, T. Moriyama, T. Ono, and Y. Tserkovnyak, *Rev. Mod. Phys.* **90**, 015005 (2018).
- [11] A. Manchon, I. M. Miron, T. Jungwirth, J. Sinova, J. Železný, A. Thiaville, K. Garello, and P. Gambardella, arXiv e-prints (2018), arXiv:1801.09636.
- [12] P. Wadley, B. Howells, J. Elezny, C. Andrews, V. Hills, R. P. Campion, V. Novak, K. Olejnik, F. Maccherozzi, S. S. Dhesi, S. Y. Martin, T. Wagner, J. Wunderlich, F. Freimuth, Y. Mokrousov, J. Kune, J. S. Chauhan, M. J. Grzybowski, A. W. Rushforth, K. W. Edmonds, B. L. Gallagher, and T. Jungwirth, *Science* **351**, 587 (2016).
- [13] H. V. Gomonay and V. M. Loktev, *Phys. Rev. B* **81**, 144427 (2010).
- [14] T. Moriyama, K. Oda, T. Ohkochi, M. Kimata, and T. Ono, *Sci. Rep.* **8**, 14167 (2018).
- [15] T. Moriyama, W. Zhou, T. Seki, K. Takanashi, and T. Ono, *Phys. Rev. Lett.* **121**, 167202 (2018).
- [16] T. Kosub, M. Koppe, R. Hühne, P. Appel, B. Shields, P. Maletinsky, R. Hübner, M. O. Liedke, J. Fassbender, O. G. Schmidt, and D. Makarov, *Nat. Commun.* **8**, 13985 (2017).

- (2017).
- [17] Y. Yanase, *J. Phys. Soc. Jpn.* **83**, 014703 (2014).
- [18] J. Železný, H. Gao, K. Výborný, J. Zemen, J. Mašek, A. Manchon, J. Wunderlich, J. Sinova, and T. Jungwirth, *Phys. Rev. Lett.* **113**, 157201 (2014).
- [19] S. Y. Bodnar, L. Šmejkal, I. Turek, T. Jungwirth, O. Gomonay, J. Sinova, A. A. Sapozhnik, H.-J. Elmers, M. Kläui, and M. Jourdan, *Nat. Commun.* **9**, 348 (2018).
- [20] M. H. Fischer, F. Loder, and M. Sigrist, *Phys. Rev. B* **84**, 184533 (2011).
- [21] X. Zhang, Q. Liu, J.-W. Luo, A. J. Freeman, and A. Zunger, *Nat. Phys.* **10**, 387 (2014).
- [22] C. Ciccarelli, L. Anderson, V. Tshitoyan, A. J. Ferguson, F. Gerhard, C. Gould, L. W. Molenkamp, J. Gayles, J. Železný, L. Šmejkal, Z. Yuan, J. Sinova, F. Freimuth, and T. Jungwirth, *Nat. Phys.* **12**, 855 (2016).
- [23] P. A. Frigeri, *Superconductivity in crystals without an inversion center*, Ph.D. thesis, ETH Zürich (2005).
- [24] D. Maruyama, M. Sigrist, and Y. Yanase, *J. Phys. Soc. Jpn.* **81**, 034702 (2012).
- [25] V. M. Edelstein, *Solid State Commun.* **73**, 233 (1990).
- [26] I. Garate and A. H. MacDonald, *Phys. Rev. B* **80**, 134403 (2009).
- [27] A. Manchon and S. Zhang, *Phys. Rev. B* **78**, 212405 (2008).
- [28] A. Manchon and S. Zhang, *Phys. Rev. B* **79**, 094422 (2009).
- [29] S. Hayami, H. Kusunose, and Y. Motome, *Phys. Rev. B* **90**, 024432 (2014).
- [30] J. Železný, H. Gao, A. Manchon, F. Freimuth, Y. Mokrousov, J. Zemen, J. Mašek, J. Sinova, and T. Jungwirth, *Phys. Rev. B* **95**, 014403 (2017).
- [31] H. Watanabe and Y. Yanase, *Phys. Rev. B* **96**, 064432 (2017).
- [32] T. Inui, Y. Tanabe, and Y. Onodera, *Group theory and its applications in physics*, Vol. Springer Series in Solid-State Sciences Vol. 78 (Springer, Berlin, 1990).
- [33] E. F. Bertaut, *Acta Crystallogr. Sect. A* **24**, 217 (1968).
- [34] Y. A. Izyumov, R. Ozerov, and V. Naish, *Neutron diffraction of magnetic materials* (Springer, Berlin, 1991).
- [35] See Supplemental Material for details of group-theoretical techniques and list of candidate materials.
- [36] H. Ohno, *Science* **281**, 951 (1998).
- [37] A. Chernyshov, M. Overby, X. Liu, J. K. Furdyna, Y. Lyanda-Geller, and L. P. Rokhinson, *Nat. Phys.* **5**, 656 (2009).
- [38] S. Esmaeilzadeh, U. Hålenius, and M. Valldor, *Chem. Mater.* **18**, 2713 (2006).
- [39] M. Seemann, D. Ködderitzsch, S. Wimmer, and H. Ebert, *Phys. Rev. B* **92**, 155138 (2015).
- [40] R. R. Birss *et al.*, *Symmetry and magnetism*, Vol. 863 (North-Holland Amsterdam, 1964).
- [41] A. P. Cracknell, *Magnetism in crystalline materials: applications of the theory of groups of cambiant symmetry* (Elsevier, Amsterdam, 2016).
- [42] N. A. Spaldin, M. Fiebig, and M. Mostovoy, *J. Phys. Condens. Matter* **20**, 434203 (2008).
- [43] H. Watanabe and Y. Yanase, *Phys. Rev. B* **98**, 245129 (2018).
- [44] K. Aizu, *Phys. Rev.* **146**, 423 (1966).
- [45] K. Aizu, *J. Phys. Soc. Jpn.* **27**, 387 (1969).
- [46] K. Aizu, *Phys. Rev. B* **2**, 754 (1970).
- [47] H. Schmid, *Ferroelectrics* **221**, 9 (1999).
- [48] H. Schmid, *J. Phys. Condens. Matter* **20**, 434201 (2008).
- [49] D. B. Litvin, *Acta Crystallogr. Sect. A Found. Crystallogr.* **64**, 316 (2008).
- [50] J. Hlinka, J. Privratska, P. Ondrejko, and V. Janovec, *Phys. Rev. Lett.* **116**, 177602 (2016).
- [51] S. A. Kimber, A. H. Hill, Y.-Z. Zhang, H. O. Jeschke, R. Valentí, C. Ritter, I. Schellenberg, W. Hermes, R. Pöttgen, and D. N. Argyriou, *Physical Review B* **82**, 100412 (2010).
- [52] A. Marcinkova, T. C. Hansen, C. Curfs, S. Margadonna, and J. W. G. Bos, *Phys. Rev. B* **82**, 174438 (2010).
- [53] N. Emery, E. J. Wildman, J. M. S. Skakle, A. C. Mclaughlin, R. I. Smith, and A. N. Fitch, *Phys. Rev. B* **83**, 144429 (2011).
- [54] Z. Fisk, M. B. Maple, D. C. Johnston, and L. D. Woolf, *Solid State Commun.* **39**, 1189 (1981).
- [55] G. Will and W. Schafer, *J. Less-Common Met.* **67**, 31 (1979).
- [56] S. Ji, C. Song, J. Koo, J. Park, Y. J. Park, K.-B. Lee, S. Lee, J.-G. Park, J. Y. Kim, B. K. Cho, K.-P. Hong, C.-H. Lee, and F. Iga, *Phys. Rev. Lett.* **99**, 076401 (2007).
- [57] G. Will, W. Schäfer, F. Pfeiffer, F. Elf, and J. Etourneau, *J. Less-Common Met.* **82**, 349 (1981).
- [58] V. M. T. S. Barthem, C. V. Colin, H. Mayaffre, M.-H. Julien, and D. Givord, *Nat. Commun.* **4**, 2892 (2013).
- [59] G. Venturini, B. Malaman, G. Le Caër, and D. Fruchart, *Phys. Rev. B* **35**, 7038 (1987).
- [60] M. Armbrüster, W. Schnelle, R. Cardoso-Gil, and Y. Grin, *Chem. - A Eur. J.* **16**, 10357 (2010).
- [61] P. Wadley, V. Novák, R. Campion, C. Rinaldi, X. Martí, H. Reichlová, J. Železný, J. Gazquez, M. Roldan, M. Varela, D. Khalyavin, S. Langridge, D. Kriegner, F. Máca, J. Mašek, R. Bertacco, V. Holý, A. Rushforth, K. Edmonds, B. Gallagher, C. Foxon, J. Wunderlich, and T. Jungwirth, *Nat. Commun.* **4**, 2322 (2013).
- [62] M. Pasturel, O. Tougait, M. Potel, T. Roisnel, K. Wochowski, H. Noël, and R. Troć, *J. Phys. Condens. Matter* **21**, 125401 (2009).
- [63] R. Troć, M. Pasturel, O. Tougait, A. P. Sazonov, A. Gukasov, C. Sułkowski, and H. Noël, *Phys. Rev. B* **85**, 064412 (2012), although this paper mentioned that the magnetic order is identified as the Γ_{12} (E_{2u}) mode, the A_{2u} mode should be admixed to realize the magnetic structure in Fig. 3 of the paper.
- [64] Q. D. Gibson, H. Wu, T. Liang, M. N. Ali, N. P. Ong, Q. Huang, and R. J. Cava, *Phys. Rev. B* **91**, 085128 (2015).
- [65] N. S. Sangeetha, V. Smetana, A.-V. Mudring, and D. C. Johnston, *Phys. Rev. B* **97**, 014402 (2018).
- [66] L. Tan, A. Kreyssig, J. W. Kim, A. I. Goldman, R. J. McQueeney, D. Wermeille, B. Sieve, T. A. Lograsso, D. L. Schlagel, S. L. Budko, V. K. Pecharsky, and K. A. Gschneidner, *Phys. Rev. B* **71**, 214408 (2005).
- [67] E. M. Levin, V. K. Pecharsky, K. A. Gschneidner, and G. J. Miller, *Phys. Rev. B* **64**, 235103 (2001).
- [68] V. H. Tran, D. Kaczorowski, R. Troć, G. André, F. Bourée, and V. Zaremba, *Solid State Commun.* **117**, 527 (2001).
- [69] S. Suzuki and S. Nakatsuji, private communication.
- [70] G. L. J. A. Rikken, J. Fölling, and P. Wyder, *Phys. Rev. Lett.* **87**, 236602 (2001).
- [71] G. L. J. A. Rikken and P. Wyder, *Phys. Rev. Lett.* **94**, 016601 (2005).
- [72] T. Ideue, K. Hamamoto, S. Koshikawa, M. Ezawa,

- S. Shimizu, Y. Kaneko, Y. Tokura, N. Nagaosa, and Y. Iwasa, *Nat. Phys.* **13**, 578 (2017).
- [73] R. Wakatsuki, Y. Saito, S. Hoshino, Y. M. Itahashi, T. Ideue, M. Ezawa, Y. Iwasa, and N. Nagaosa, *Sci. Adv.* **3**, e1602390 (2017).
- [74] K. Yasuda, A. Tsukazaki, R. Yoshimi, K. S. Takahashi, M. Kawasaki, and Y. Tokura, *Phys. Rev. Lett.* **117**, 127202 (2016).
- [75] K. Olejník, V. Novák, J. Wunderlich, and T. Jungwirth, *Phys. Rev. B* **91**, 180402 (2015).
- [76] B. B. Van Aken, J.-P. Rivera, H. Schmid, and M. Fiebig, *Nature (London)* **449**, 702 (2007).
- [77] A. S. Zimmermann, D. Meier, and M. Fiebig, *Nat. Commun.* **5**, 4796 (2014).
- [78] J. Godinho, H. Reichlova, D. Kriegner, V. Novak, K. Olejník, Z. Kaspar, Z. Soban, P. Wadley, R. P. Champion, R. M. Otxoa, P. E. Roy, J. Zelezny, T. Jungwirth, and J. Wunderlich, *Nat. Commun.* **9**, 4686 (2018).
- [79] Y. Gao and D. Xiao, *Phys. Rev. B* **98**, 060402 (2018).

Supplemental Material: Symmetry analysis of electrical switching of antiferromagnets

S1. MAGNETIC REPRESENTATION THEORY

Here, we present a brief introduction to the representation theory for magnetic phase transitions [S1, S2] and apply the theory to the case of CuMnAs [S3, S4]. The magnetic representation, which describes symmetry of possible magnetic structures, is systematically obtained from a given crystal symmetry. A projection operator identifies the basis of the magnetic order in the way that the basis is symmetry-adapted to the irreducible representation.

A magnetic order is accompanied by the loss of some symmetry operations of a given space group \mathcal{G} . Hence, the representation analysis based on the group theory is a powerful tool to investigate possible magnetic structures. The availability has been recognized in a lot of experimental works [S2]. Here we assume magnetic structures with no translational symmetry breaking ($\mathbf{Q} = \mathbf{0}$), where the magnetic unit cell is the same as the chemical cell. In this case, the magnetic structure is invariant to every translational operation of the space group \mathcal{G} , and thus the transformation property of the basis is determined by the point group \mathbf{G} of the crystalline system. It is reasonable for the symmetry analysis of electrical switching of antiferromagnets to consider the point group symmetry, since applied external fields are uniform and cannot distinguish domain states induced by a translational symmetry breaking.

We denote by $\mathbf{m}^{(\alpha)}$ a magnetic moment localized at a crystallographic sublattice α in a unit cell. The magnetic basis $\{m_\nu^{(\alpha)}\}$ are transformed by the symmetry operation $g \in \mathbf{G}$ as

$$g \left(m_\nu^{(\alpha)} \right) = \sum_{\beta\mu} m_\mu^{(\beta)} [D^{(M)}(g)]_{\mu\nu} [D^{(P)}(g)]_{\beta\alpha}, \quad (\text{S1})$$

where $D^{(M)}$ and $D^{(P)}$ are matrices which represent the transformation property of an axial vector and sublattice permutation, respectively. Therefore, the representation of the magnetic basis is written by the direct product,

$$\Gamma_{\mathbf{G}}^{\text{mag}}(\mathbf{H}) = \Gamma_{\mathbf{G}}^{\text{P}}(\mathbf{H}) \otimes \Gamma_{\mathbf{G}}^{\text{M}}. \quad (\text{S2})$$

$\Gamma_{\mathbf{G}}^{\text{P}}$ represents the sublattice permutation representation with the site-symmetry group \mathbf{H} . $\Gamma_{\mathbf{G}}^{\text{M}}$ denotes the axial vector representation. All the magnetic structures constructed from $\{m_\nu^{(\alpha)}\}$ break the time-reversal symmetry, since the representation $\Gamma_{\mathbf{G}}^{\text{M}}$ ($\Gamma_{\mathbf{G}}^{\text{P}}$) shows the odd (even) parity under the time-reversal operation.

The symmetry-adapted basis of the magnetic order are given by irreducible representations $\{\Gamma_{\mathbf{G}}^{(a)}\}$. Now, we decompose the magnetic representation (S2) to identify which irreducible representation is comprised. The decomposition is given by

$$\Gamma_{\mathbf{G}}^{\text{mag}}(\mathbf{H}) = \sum_a q_a \Gamma_{\mathbf{G}}^{(a)}. \quad (\text{S3})$$

The independent magnetic basis of the representation $\Gamma_{\mathbf{G}}^{(a)}$ is as many as q_a . The coefficient q_a is given by

$$q_a = \frac{1}{|\mathbf{G}|} \sum_{g \in \mathbf{G}} \chi_a^*(g) \chi_{\text{mag}}(g), \quad (\text{S4})$$

where $|\mathbf{G}|$ is the order of the point group \mathbf{G} . $\chi_a(g)$ and $\chi_{\text{mag}}(g)$ are characters of the representations $\Gamma_{\mathbf{G}}^{(a)}$ and $\Gamma_{\mathbf{G}}^{\text{mag}}$, respectively. The character $\chi_{\text{mag}}(g)$ is obtained by multiplying the character of the representation $\Gamma_{\mathbf{G}}^{\text{P}}$ and that of $\Gamma_{\mathbf{G}}^{\text{M}}$ owing to Eq. (S2).

The magnetic basis of the irreducible representation $\Gamma_{\mathbf{G}}^{(a)}$, labeled by ξ , is given by the projection operator

$$\hat{P}_\xi^{(a)} = \frac{\dim \Gamma_{\mathbf{G}}^{(a)}}{|\mathbf{G}|} \sum_{g \in \mathbf{G}} [D^{(a)}(g)]_{\xi\xi}^* g, \quad (\text{S5})$$

where $\xi = 1, 2, \dots, \dim \Gamma_{\mathbf{G}}^{(a)}$. In particular, for an one-dimensional irreducible representation, the projection operator is simplified as

$$\hat{P}^{(a)} = \frac{1}{|\mathbf{G}|} \sum_{g \in \mathbf{G}} \chi_a^*(g) g, \quad (\text{S6})$$

where $\chi_a(g) = \text{Tr} D^{(a)}(g)$. Thus, we can complete all the possible magnetic structures by the representation theory technique.

A. Application to CuMnAs

We apply the representation theory to CuMnAs, where the antiferromagnetic (AFM) domain switching has been demonstrated [S3]. The compound shows a ferrotoroidic order in the AFM phase. Here, we investigate possible magnetic structures of CuMnAs and clarify the relation between the toroidal moment and the magnetic mode for the realized AFM order.

The magnetic sites, Mn atoms, are positioned at the crystallographic position with the site-symmetry group $\mathbf{H} = 4mm$, while the crystal group is $\mathbf{G} = 4/mmm$. The coset decomposition of \mathbf{G} by \mathbf{H} is obtained as,

$$\mathbf{G} = I\mathbf{H} + P\mathbf{H}, \quad (\text{S7})$$

where I and P represent the identity operation and parity operation, respectively. The number of the sublattice is the ratio $|\mathbf{G}|/|\mathbf{H}| = 2$ obtained from the coset decomposition (S7).

Now, we examine a transformation property of the sublattice permutation. The matrix element of $D^{(P)}(g)$ is given by

$$[D^{(P)}(g)]_{ab} = \delta(a, g(b)), \quad (\text{S8})$$

and $\delta(a, b)$ is defined as

$$\delta(a, b) = \begin{cases} 1 & \text{for } a = b, \\ 0 & \text{for } a \neq b, \end{cases} \quad (\text{S9})$$

which is parametrized by the sublattice indexes a and b . In the case of CuMnAs, the two sublattices are interchanged by the parity operation $g = P$. Thus, the representation matrix is given by

$$D^{(P)}(P) = \begin{pmatrix} 0 & 1 \\ 1 & 0 \end{pmatrix}, \quad (\text{S10})$$

and therefore the character is $\chi_P(P) = \text{Tr } D^{(P)}(P) = 0$. It follows that any sublattice does not return to its crystallographic position by the operation P . The condition $\chi_P(P) = 0$ represents the locally noncentrosymmetric property of Mn atoms in CuMnAs. Similarly, characters of the symmetry operation $g \in \mathbf{G}$ are obtained as in Table S1.

The characters of the axial vector representation $\chi_M(g)$ are obtained by the trace of the representation matrices of an axial vector. In the case of the group $\mathbf{G} = 4/mmm$, the character $\chi_M(g)$ is given by a summation of the characters of the A_{2g} and E_g irreducible representations. This is because the axial vector representation $\Gamma_{\mathbf{G}}^M$ is given by the direct sum of A_{2g} and E_g . In fact, magnetization M_z and $\{M_x, M_y\}$ belong to the representations A_{2g} and E_g , respectively.

TABLE S1. The character table in the crystal group $\mathbf{G} = 4/mmm$ for the representation $\Gamma_{\mathbf{G}}^P$, $\Gamma_{\mathbf{G}}^M$, and $\Gamma_{\mathbf{G}}^{\text{mag}}$. The magnetic sites are supposed to be Mn atoms of CuMnAs. The conventional notation is adopted for the symmetry operations of $\mathbf{G} = 4/mmm$ [S5].

$g \in \mathbf{G}$	E	$2C_4$	C_{2z}	$2C_2'$	$2C_2''$	P	$2S_4$	σ_h	$2\sigma_v$	$2\sigma_d$
$\chi_P(g)$	2	2	2	0	0	0	0	0	2	2
$\chi_M(g)$	3	1	-1	-1	-1	3	1	-1	-1	-1
$\chi_{\text{mag}}(g)$	6	2	-2	0	0	0	0	0	-2	-2

The coefficients $\{q_a\}$ calculated by Eq. (S4) give the decomposition of the magnetic representation as

$$\Gamma_{\mathbf{G}}^{\text{mag}}(\mathbf{H}) = A_{2g} + A_{1u} + E_g + E_u, \quad (\text{S11})$$

among which the E_u irreducible representation corresponds to the AFM order of CuMnAs [S3, S4].

The symmetry-adapted basis are obtained by the projection operator (S5). Taking the basis of the E_u representation as $\{x, y\}$, we accordingly obtain matrix elements of the representation matrix $D^{(E_u)}$ in Eq. (S5). The projection operator for the $E_u(x)$ basis identifies the magnetic structure

$$\mathbf{m}^{(1)} = m\hat{y}, \quad \mathbf{m}^{(2)} = -m\hat{y}, \quad (\text{S12})$$

where $\mathbf{m}^{(1)}$ and $\mathbf{m}^{(2)}$ represent magnetic moments localized at the two sublattices. The toroidal moment $T_0\hat{x}$ also belongs to the $E_u(x)$ basis, and hence the magnetic structure (S12) is induced by the electric current $\mathbf{j} \parallel \hat{x}$. Similarly, we obtain the the magnetic structure belonging to the $E_u(y)$ basis as

$$\mathbf{m}^{(1)} = -m\hat{x}, \quad \mathbf{m}^{(2)} = m\hat{x}, \quad (\text{S13})$$

which corresponds to the toroidal moment $T_0\hat{y}$. The result of the representation analysis is consistent with the microscopic study for the AFM Edelstein effect [S6].

Note that we may obtain the irreducible decomposition of $\Gamma_{\mathbf{G}}^{\text{P}}$ without making use of the permutation matrices such as Eq. (S10). The definition (S8) says that the permutation representation is the induced representation of the identity representation $\Gamma_{\mathbf{H}}^{(1)}$ on the group \mathbf{G} ,

$$\Gamma_{\mathbf{G}}^{\text{P}}(\mathbf{H}) = \Gamma_{\mathbf{H}}^{(1)} \uparrow \mathbf{G} = \sum_a p_a \Gamma_{\mathbf{G}}^{(a)}, \quad (\text{S14})$$

In general, irreducible representations $\{\Gamma_{\mathbf{G}}^{(a)}\}$ are reducible in the subgroup $\mathbf{H} (\subset \mathbf{G})$, and hence those representations are decomposed by the irreducible representations of \mathbf{H} as

$$\Gamma_{\mathbf{G}}^{(a)} \downarrow \mathbf{H} = \sum_b p_b' \Gamma_{\mathbf{H}}^{(b)}. \quad (\text{S15})$$

Following the Frobenius reciprocity [S5], a useful formula is obtained as

$$p_a = p_1'^{(a)}, \quad (\text{S16})$$

where the right-hand-side is obtained by the compatibility relation between the groups \mathbf{G} and \mathbf{H} . In the case of CuMnAs ($\mathbf{G} = 4/mmm$, $\mathbf{H} = 4mm$), the compatibility of the irreducible representation is shown in Table S2. Therefore, the coefficients in Eq. (S14) are obtained as

$$p_a = \begin{cases} 1 & \text{for } a = A_{1g}, A_{2u}, \\ 0 & \text{otherwise.} \end{cases} \quad (\text{S17})$$

Thus, $\Gamma_{\mathbf{G}}^{\text{P}}$ is given by

$$\Gamma_{\mathbf{G}}^{\text{P}} = A_{1g} + A_{2u}. \quad (\text{S18})$$

As demonstrated above, the irreducible decomposition of $\Gamma_{\mathbf{G}}^{\text{P}}$ is determined by only the compatibility relation between \mathbf{G} and \mathbf{H} . Accordingly, with the use of product rules for the irreducible representations we obtain $\Gamma_{\mathbf{G}}^{\text{mag}}$ as

$$\Gamma_{\mathbf{G}}^{\text{mag}}(\mathbf{H}) = \Gamma_{\mathbf{G}}^{\text{P}}(\mathbf{H}) \otimes \Gamma_{\mathbf{G}}^{\text{M}}, \quad (\text{S19})$$

$$= (A_{1g} + A_{2u}) \otimes (A_{2g} + E_g), \quad (\text{S20})$$

$$= A_{2g} + E_g + A_{1u} + E_u, \quad (\text{S21})$$

which is the same result as Eq. (S11).

TABLE S2. The compatibility relation of the irreducible representations of $\mathbf{G} = 4/mmm$ in the case of the symmetry reduction $\mathbf{G} = 4/mmm \rightarrow \mathbf{H} = 4mm$. The A_1 irreducible representation is the identity representation of the group $4mm$.

$\Gamma_{\mathbf{G}}$	A_{1g}	A_{2g}	B_{1g}	B_{2g}	E_g	A_{1u}	A_{2u}	B_{1u}	B_{2u}	E_u
$\Gamma_{\mathbf{G}} \downarrow \mathbf{H}$	A_1	A_2	B_1	B_2	E	A_2	A_1	B_2	B_1	E

S2. EXTENSION TO NONCENTROSYMMETRIC SYSTEMS

Our symmetry analysis can be straightforwardly extended to ferromagnetic or AFM order in noncentrosymmetric systems, while in the main text we focus on the AFM order in centrosymmetric crystalline systems. In this section,

we introduce a symmetry analysis based on the Aizu species and the representation theory in noncentrosymmetric systems, and apply the extended scheme to strained (Ga,Mn)As and MnSiN₂ as examples of switchable magnets with noncentrosymmetric crystalline structures.

The Aizu species analysis is extended in a straightforward way. When the system undergoes the magnetic phase transition which is switchable by the electric current, its species should be full or partial toroidal. Thus, the presence of the toroidal moment is a criterion of the electrical switching, irrespective of whether the crystalline structure is centrosymmetric or noncentrosymmetric. An important difference of noncentrosymmetric systems from centrosymmetric systems is the following. The species of switchable magnets can be full-magnetic, that is, magnetic structures can be ferromagnetic, since the \mathcal{PT} symmetry is absent in the noncentrosymmetric systems. A switchable domain state may comprise ferromagnetic moment in addition to the toroidal moment.

As for the representation analysis of noncentrosymmetric systems, we obtain possible magnetic basis in the same manner as in Appendix S1. By supposing magnetic sites with site-symmetry group \mathbf{H} , magnetic representation of crystal group \mathbf{G} is obtained as Eq. (S2). The parity of each magnetic basis cannot be determined anymore owing to the fact that \mathbf{G} is noncentrosymmetric. Below we discuss ferromagnet and antiferromagnet on the basis of the representation theory.

First, we present the criterion for the current-induced switching of ferromagnets. In contrast to centrosymmetric systems, the (ferromagnetic) Edelstein effect is allowed in noncentrosymmetric crystals [S7, S8]. The formula for the Edelstein effect is written as

$$M_\mu = \kappa_{\mu\nu}^{\text{FM}} j_\nu, \quad (\text{S22})$$

where the susceptibility tensor has no sublattice degree of freedom in contrast to the AFM Edelstein effect [Eq. (3) in the main text]. The magnetic representation of the ferromagnetic order is same as the axial vector representation,

$$\Gamma_{\mathbf{G}}^{\text{FM}} = \Gamma_{\mathbf{G}}^{\mathbf{M}} \subset \Gamma_{\mathbf{G}}^{\text{mag}}(\mathbf{H}), \quad (\text{S23})$$

which is obtained by replacing the permutation representation $\Gamma_{\mathbf{G}}^{\mathbf{P}}$ in Eq. (S2) with the identity representation $\Gamma_{\mathbf{G}}^{(1)}$.

Here we impose the symmetry of a paramagnetic state on the susceptibility $\kappa_{\mu\nu}^{\text{FM}}$. The symmetry operations $g \in \mathbf{G}$ give constraints to the susceptibility tensor $\kappa_{\mu\nu}^{\text{FM}}$ in accordance with Neumann's principle. The representation of the susceptibility $\kappa_{\mu\nu}^{\text{FM}}$ is decomposed as

$$\Gamma_{\mathbf{G}}^{\text{FM}} \otimes \Gamma_{\mathbf{G}}^{\mathbf{j}} = \sum_{\alpha} p_{\alpha} \Gamma_{\mathbf{G}}^{(\alpha)}, \quad (\text{S24})$$

where p_1 for the identity representation $\Gamma_{\mathbf{G}}^{(1)}$ gives the number of independent coefficients of the tensor $\kappa_{\mu\nu}^{\text{FM}}$. The condition $p_1 \neq 0$ can be represented by

$$\sum_{g \in \mathbf{G}} \chi_{\mathbf{j}}^*(g) \chi_{\text{FM}}(g) \neq 0, \quad (\text{S25})$$

due to Eq. (S4). $\chi_{\mathbf{j}}(g)$ and $\chi_{\text{FM}}(g)$ are the character of the representations $\Gamma_{\mathbf{G}}^{\mathbf{j}}$ and $\Gamma_{\mathbf{G}}^{\text{FM}}$, respectively.

The ferromagnetic representation should share the same irreducible representation with the polar vector representation $\Gamma_{\mathbf{G}}^{\mathbf{j}}$ when the ferromagnetic order is induced by the electric current \mathbf{j} . In other words, the ferromagnetic representation should comprise the toroidal moment representation which is the same as $\Gamma_{\mathbf{G}}^{\mathbf{j}}$. Thus, the toroidal moment is necessary for the current-induced ferromagnetic domain switching, although the attention was not paid in the spintronics studies. The crystal groups, where the Edelstein effect is allowed, are called as gyrotropic [S7].

Next, we show the criterion for the switching of antiferromagnets. The representation of AFM order is obtained by subtracting the ferromagnetic representation $\Gamma_{\mathbf{G}}^{\text{FM}}$ from the magnetic representation $\Gamma_{\mathbf{G}}^{\text{mag}}$ owing to the relation,

$$\Gamma_{\mathbf{G}}^{\text{mag}}(\mathbf{H}) = \Gamma_{\mathbf{G}}^{\text{FM}} + \Gamma_{\mathbf{G}}^{\text{AFM}}(\mathbf{H}). \quad (\text{S26})$$

Similarly, the representation of the AFM Edelstein susceptibility is decomposed as

$$\Gamma_{\mathbf{G}}^{\text{AFM}}(\mathbf{H}) \otimes \Gamma_{\mathbf{G}}^{\mathbf{j}} = \sum_{\alpha} r_{\alpha} \Gamma_{\mathbf{G}}^{(\alpha)}. \quad (\text{S27})$$

The AFM Edelstein effect is allowed when satisfying $r_1 \neq 0$. The condition $r_1 \neq 0$ can be recast

$$\sum_{g \in \mathbf{G}} \chi_{\mathbf{j}}^*(g) [\chi_{\text{mag}}(g) - \chi_{\text{FM}}(g)] \neq 0, \quad (\text{S28})$$

which is derived from Eq. (S26). In the case of $r_1 \neq 0$, the AFM representation comprises the toroidal moment representation, that is, $\Gamma_{\mathbf{G}}^j$. The toroidal moment which a realized AFM state comprises is inverted to be parallel to the injected electric current. Thus, the criterion is the same as that for the switching of ferromagnets.

In the following, we discuss two examples: strained (Ga,Mn)As is a noncentrosymmetric ferromagnet whereas MnSiN₂ is a noncentrosymmetric antiferromagnet.

A. Strained (Ga,Mn)As

(Ga,Mn)As is a ferromagnetic semiconductor, crystallizing in the zinc-blende structure [S9]. Let us assume that the magnetic atoms (Mn) are positioned at Ga sites. The magnetic sites have no sublattice degree of freedom, and the magnetic representation is obtained as

$$\Gamma_{\mathbf{G}}^{\text{mag}}(\mathbf{H}) = \Gamma_{\mathbf{G}}^{\text{FM}} = \Gamma_{\mathbf{G}}^M. \quad (\text{S29})$$

The Edelstein effect is not allowed in (Ga,Mn)As, since the crystal group of the zinc-blende structure is $\mathbf{G} = \bar{4}3m$ which is noncentrosymmetric but non-gyrotropic. In fact, the magnetic representation (S29) given by $\Gamma_{\mathbf{G}}^{\text{mag}} = T_1$ differs from the polar vector representation $\Gamma_{\mathbf{G}}^j = T_2$. Thus, the criterion for the switching magnetic domain is not satisfied.

Now, we suppose that the crystal structure is deformed from cubic to tetragonal by applying strain represented by ϵ_{zz} . Accordingly, the crystal group is transformed into $\mathbf{G}' = \bar{4}2m$. The applied strain also reduces the representations of axial and polar vectors as

$$\begin{aligned} \Gamma_{\mathbf{G}}^M \downarrow \mathbf{G}' &= A_2 + E, \\ \Gamma_{\mathbf{G}}^j \downarrow \mathbf{G}' &= B_2 + E, \end{aligned} \quad (\text{S30})$$

where we use the compatibility relation between \mathbf{G} and \mathbf{G}' . The representations $\Gamma_{\mathbf{G}}^{\text{mag}} (= \Gamma_{\mathbf{G}}^M)$ and $\Gamma_{\mathbf{G}}^j$ comprise the same representation E . Therefore, $p_1 = 1$ in Eq. (S24), since the identity representation $\Gamma_{\mathbf{G}'}^{(1)} = A_1$ is obtained from the product representation $E \otimes E$. Indeed, the product is decomposed as

$$E \otimes E = A_1 + A_2 + B_1 + B_2. \quad (\text{S31})$$

Thus, the Edelstein effect is allowed in the strained system. In other words, the crystal group is changed from non-gyrotropic into gyrotropic by applying the strain.

By using the projection operator associated with the E irreducible representation, the ferromagnetic moment M_x and M_y are identified to be symmetry-adapted to the electric current j_y and j_x , respectively. When the ferromagnetic moment $M_x > 0$ is induced by the electric current $j_y > 0$, $M_y > 0$ has to be induced by $j_x > 0$ because of the fourfold improper rotations of \mathbf{G}' . The elements of the tensor $\kappa_{\mu\nu}^{\text{FM}}$ are given by

$$\begin{cases} \kappa_{xy}^{\text{FM}} = \kappa_{yx}^{\text{FM}} \neq 0, \\ \kappa_{\mu\nu}^{\text{FM}} = 0 \end{cases} \quad (\mu, \nu) \text{ for otherwise.} \quad (\text{S32})$$

This form of the susceptibility corresponds to the Dresselhaus-type spin-momentum coupling [S10].

We also perform symmetry analysis based on the Aizu species. When the ferromagnetic moment is aligned along the x axis in the strain-free (Ga,Mn)As, the species and its property are obtained as

$$\begin{array}{c} \hline \hline \bar{4}3m1' \ F\bar{4}2'm' \ \hat{\epsilon} \ \mathbf{P} \ \mathbf{M} \ \mathbf{T} \\ \mathbf{P} \ \mathbf{Z} \ \mathbf{F} \ \mathbf{Z} \\ \hline \hline \end{array}$$

The species is full magnetic and zero toroidal. It turns out that the ferromagnetic moment of the unstrained (Ga,Mn)As is not switchable by the electric current, while it can be inverted by the magnetic field.

On the other hand, the species of a strained system with in-plane ferromagnetic moment is described by

$$\begin{array}{c} \hline \hline \bar{4}2m1' \ F2'2'2 \langle x \rangle \ \hat{\epsilon} \ \mathbf{P} \ \mathbf{M} \ \mathbf{T} \\ \mathbf{P} \ \mathbf{Z} \ \mathbf{F} \ \mathbf{F} \\ \hline \hline \end{array}$$

where $\langle x \rangle$ indicates that the twofold rotation axis is the x or y axis. The species of the strained (Ga,Mn)As turns into full toroidal species. Thus, the in-plane ferromagnetic order is perfectly controllable not only by the magnetic field but also by the electric current. The Aizu species analysis is consistent with the representation analysis.

where we suppose $\mathbf{P}_0 \parallel \hat{z}$ without loss of generality. The domains are related with each other as

$$s_2 = \theta s_1, \quad s_3 = C_{2x} s_1, \quad s_4 = \theta C_{2x} s_1. \quad (\text{S38})$$

The domains connected by the time-reversal operation θ cannot be distinguished by the electric polarization \mathbf{P} . Thus, the species should be characterized as partial electric in the rigorous sense. Especially, it is important for our symmetry analysis of the switchable antiferromagnets to distinguish the domains connected by the operation θ , since those domains may be discerned by the toroidal moment and inverted by applying the electric current.

S4. PARTIAL TOROIDIC PROPERTY OF MAGNETIC HONEYCOMB LATTICE

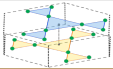
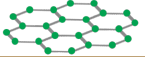
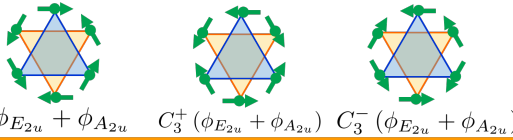
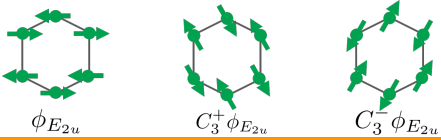
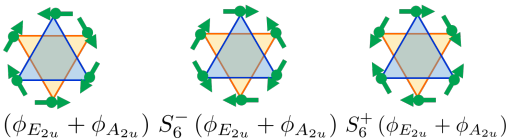
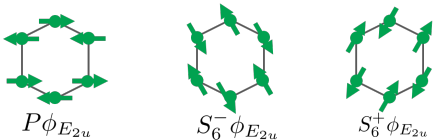
	$\text{U}_3\text{Ru}_4\text{Al}_{12}$ 	2D-honeycomb 
$+T_z$	 $\phi_{E_{2u}} + \phi_{A_{2u}}$ $C_3^+(\phi_{E_{2u}} + \phi_{A_{2u}})$ $C_3^-(\phi_{E_{2u}} + \phi_{A_{2u}})$	 $\phi_{E_{2u}}$ $C_3^+\phi_{E_{2u}}$ $C_3^-\phi_{E_{2u}}$
$-T_z$	 $P(\phi_{E_{2u}} + \phi_{A_{2u}})$ $S_6^-(\phi_{E_{2u}} + \phi_{A_{2u}})$ $S_6^+(\phi_{E_{2u}} + \phi_{A_{2u}})$	 $P\phi_{E_{2u}}$ $S_6^-\phi_{E_{2u}}$ $S_6^+\phi_{E_{2u}}$

FIG. S1. The magnetic domains of $\text{U}_3\text{Ru}_4\text{Al}_{12}$ [S14] (left panels) and two-dimensional honeycomb lattice (right panels). C_3^\pm (S_6^\pm) denotes the threefold rotation (rotatory inversion) operation. $\text{U}_3\text{Ru}_4\text{Al}_{12}$ has a toroidal moment, $\pm T\hat{z}$, while it vanishes in the honeycomb lattice without taking the magnetostrictive effect into account.

In this section, we consider a fictitious example of a partial toroidic species: a collinear AFM order of a honeycomb lattice. By comparing the honeycomb lattice to $\text{U}_3\text{Ru}_4\text{Al}_{12}$, which also belongs to a partial toroidic species, we illuminate a complementary role of the representation analysis and the Aizu species analysis.

Let us assume that the honeycomb lattice (the crystal group $\mathbf{G} = 6/mmm$), hosting two sublattices with the site-symmetry group $\mathbf{H} = \bar{6}2m$, undergoes a collinear AFM order aligned along the twofold axis in the xy plane as shown in the right panels of Fig S1. Such magnetic order may realize in magnetic honeycomb systems such as transition-metal trichalcogenides [S15, S16].

The assumed AFM order belongs to the same Aizu species as that of $\text{U}_3\text{Ru}_4\text{Al}_{12}$ [Eq. (14) in the main text]. Therefore, we may expect that the domains are partially-controllable by the electric current j_z as in the case of $\text{U}_3\text{Ru}_4\text{Al}_{12}$. The magnetic representation theory of the honeycomb lattice, however, leads to

$$\Gamma_{\mathbf{G}}^{\text{mag}}(\mathbf{H}) = A_{2g} + E_{1g} + B_{2u} + E_{2u}, \quad (\text{S39})$$

which do not comprise the polar representation $\Gamma_{\mathbf{G}}^j = A_{2u} + E_{1u}$ in contrast to the magnetic representation of $\text{U}_3\text{Ru}_4\text{Al}_{12}$ [Eq. (15) in the main text]. As shown in Fig. S1, the AFM structure of the honeycomb lattice actually contains only a nonpolar mode obtained as the E_{2u} mode, while the AFM order of $\text{U}_3\text{Ru}_4\text{Al}_{12}$ is represented by a polar mode, that is, the A_{2u} mode in addition to the E_{2u} mode. Then, the current j_z is not linearly coupled to the AFM order. Thus, the AFM domains of the honeycomb lattice are not switchable by the AFM Edelstein effect.

The criterion for the controllability, that is, whether the AFM order comprises a toroidic moment depends on the site-symmetry of magnetic sites in a partial toroidic species. The representation theory and the Aizu species analysis are complementary: The presence or absence of a toroidal moment in an AFM state should be checked by the representation analysis, while the controllability of domains is understood by the Aizu species analysis.

To keep the consistency between the Aizu species analysis and the representation theory analysis as for the honeycomb lattice, we need to consider a magnetostrictive effect. In Eq. (S39), we assume that the magnetic representation is determined by the crystalline structure in the paramagnetic phase. A magnetic phase transition, however, may give rise to a structural change through a magnetic-elastic coupling, namely, magnetostrictive effect. The structural change transforms the magnetic representation into that in a lowered crystal symmetry.

Now, we consider the AFM phase which has the polar axis along the z axis and the mirror symmetry for the zx plane. Owing to the magnetostrictive effect, the strain $\epsilon_{xx} - \epsilon_{yy}$ is induced by the AFM order. This is phenomenologically understood by the Landau's free energy,

$$\mathcal{F} = a\eta_{\text{AF}}^2 + c\eta_{\text{AF}}^4 + \lambda\eta_{\text{AF}}^2\eta_\epsilon + \dots, \quad (\text{S40})$$

where η_{AF} and η_ϵ represent the AFM order parameter and the induced strain. λ represents the magneto-elastic coupling. When the AFM phase transition occurs with a non-negligible coupling λ , the crystal structure is deformed from hexagonal to orthorhombic as $\mathbf{G} = 6/mmm$ to $\mathbf{G}' = mmm$. Similarly, the site-symmetry group of the sublattice is transformed as $\mathbf{H} = \bar{6}2m$ to $\mathbf{H}' = 2mm$. The magnetic representation of the honeycomb lattice is reduced from Eq. (S39) to

$$\Gamma_{\mathbf{G}'}^{\text{mag}}(\mathbf{H}') = B_{1g} + (B_{2g} + B_{3g}) + B_{2u} + (A_u + B_{1u}). \quad (\text{S41})$$

The E_{2u} irreducible representation becomes reducible in the descended group \mathbf{G}' , and the irreducible decomposition is given by

$$E_{2u} \downarrow \mathbf{G}' = A_u + B_{1u}. \quad (\text{S42})$$

The toroidal moment $\mathbf{T} \parallel \hat{z}$ belongs to the B_{1u} irreducible representation of \mathbf{G}' , and thus the electric current j_z can control the AFM state through the AFM Edelstein effect induced by the magnetostrictive effect.

Although the current-induced switching is possible in other AFM domains in a similar manner, the magnetically-induced strains in the xy plane are not coupled to the out-of-plane electric current j_z . Therefore, the switching of AFM domains having the same toroidal moment cannot be caused by the electric current. This is consistent with the partial toroidic property of the Aizu species. As shown above, by taking the magnetostrictive effect into account, the representation analysis is consistent with the Aizu species analysis in the case of the honeycomb lattice.

S5. MAGNETOPIEZOELECTRIC EFFECT

In this section, we propose switching of magnetic states by a combination of the electric current and stress. This is similar to switching of structural deformations by making use of the piezoelectric effect, which is the coupling between the electric field and strain. In the following, we introduce a magnetopiezoelectric effect, and discuss the switching of magnetic compounds by using the magnetopiezoelectric effect.

First, let us consider how we manipulate domains of a metallic antiferromagnet $\text{U}_3\text{Ru}_4\text{Al}_{12}$ [S14]. The species of $\text{U}_3\text{Ru}_4\text{Al}_{12}$ is denoted as

$$6/mmm1' Fmmm' \langle z \rangle, \quad (\text{S43})$$

property of which is described as follows [Table III in the main text].

$6/mmm1' Fmmm' \langle z \rangle$	$\hat{\epsilon}$	\mathbf{P}	\mathbf{M}	\mathbf{T}
	\mathbf{P}	\mathbf{Z}	\mathbf{Z}	\mathbf{P}

This implies that none of the physical quantities (strain $\hat{\epsilon}$, electric polarization \mathbf{P} , ferromagnetic moment \mathbf{M} , and toroidal moment \mathbf{T}) distinguish the domain states of $\text{U}_3\text{Ru}_4\text{Al}_{12}$ in the complete way. The magnetopiezoelectricity derived from asymmetric distortions of the electronic band structure, however, may be useful for the perfect distinction of the AFM domains [S17, S18].

Next, we introduce the magnetopiezoelectric effect. The asymmetric dispersion in the energy spectrum is realized in systems where both of the parity and time-reversal symmetries are broken. The antisymmetric part in the energy dispersion leads to an electronic nematicity under an electric current. For example, in a system with an asymmetric dispersion which is symmetry-adapted to the basis $k_x k_y k_z$, the electric current j_z gives rise to the electronic nematic order in the $k_x k_y$ plane. Accordingly, the electronic nematicity induces an ionic displacement, that is, the strain represented by ϵ_{xy} . The coupling between the electric current and the electronic/ionic nematic order is called magnetopiezoelectricity [S17], since the time-reversal symmetry breaking is necessary.

The sign of the magnetopiezoelectric effect differs between the AFM domains connected by the operation θ . Thus, the AFM domains of $\text{U}_3\text{Ru}_4\text{Al}_{12}$ are completely distinguished by the magnetopiezoelectric effect, and the Aizu species can be classified as full magnetopiezoelectric species. In order words, the AFM domains are perfectly manipulated

by making use of the electric current and stress. Although the electric current j_z can switch the domains only in an incomplete way as discussed in the main text, the stress can control the magnetostrictive strains and therefore manipulate the domains with the same toroidal moment $\mathbf{T} \parallel \hat{z}$. Thus, combination of the electric current and stress enables the perfect AFM domain switching.

The full magnetopiezoelectric property is satisfied in most of the zero toroidal species when both of the space-inversion and time-reversal symmetries are broken. Hence, the zero toroidal magnetic compounds may be manipulated by applying the electric current and stress, while domains cannot be inverted by only the electric current because of an absence of the ferrotoroidal order. It should be noticed that the strain-free (Ga,Mn)As discussed in Sec. S2 A is zero toroidal but full magnetopiezoelectric, and the ferromagnetic domains can be manipulated by a combined use of the electric current and stress [S10].

S6. CANDIDATE MATERIALS FOR ELECTRICAL SWITCHING OF ANTIFERROMAGNETIC ORDER

Our symmetry analysis uncovers a lot of candidate materials for electrically switchable antiferromagnets besides CuMnAs and Mn₂Au [S4, S19]. In the following, we discuss some candidate materials we identified with a focus on the \mathcal{PT} -symmetric and $\mathbf{Q} = \mathbf{0}$ magnetic states. At the end of this section, we also show the list of more than 50 candidate materials.

A. BaMn₂As₂ and CeMn₂Ge₂

BaMn₂As₂ and CeMn₂Si₂ crystallize in a tetragonal structure, which is a well-known ThCr₂Si₂-type structure (space group: $I4/mmm$, No. 139). Both compounds undergo the AFM phase transitions [S20–S22] and the corresponding Aizu species are given by

$$4/mmm1' F4'/m'm'm \text{ (} z\text{-collinear AFM)}, \quad (\text{S44})$$

for BaMn₂As₂, and

$$4/mmm1' Fmmm' \langle x \rangle \text{ (} x\text{-, } y\text{-collinear AFM)}, \quad (\text{S45})$$

for CeMn₂Si₂. The former species is zero toroidal, and the AFM state is not controllable by the electric current \mathbf{j} . On the other hand, the latter species is the same as CuMnAs, that is, full toroidal species indicating the AFM state perfectly controllable by \mathbf{j} .

The above classification is supported by the representation analysis. The magnetic sites Mn are characterized by the site-symmetry group $\mathbf{H} = \bar{4}m2$. The magnetic representation is obtained as

$$\Gamma_{\mathbf{G}}^{\text{mag}}(\mathbf{H}) = A_{2g} + E_g + B_{1u} + E_u. \quad (\text{S46})$$

The AFM states of BaMn₂As₂ and CeMn₂Si₂ are characterized by the B_{1u} and the E_u irreducible representation, respectively. While the former irreducible representation is nonpolar, the latter is polar and comprises the in-plane toroidal moment $\{T_x, T_y\}$ in its basis. Thus, although the AFM order of BaMn₂As₂ cannot be controlled by an electric current, the AFM order of CeMn₂Si₂ is switchable by the in-plane electric current as in the case of CuMnAs. Therefore, CeMn₂Si₂ and related materials may be a new electrically switchable antiferromagnets.

B. Trigonal XMn₂Pn₂

Some Mn 122-compounds denoted by the chemical formula XMn₂Pn₂ crystallize in a trigonal structure (space group: $P\bar{3}m1$, No. 164) which is different from the ThCr₂Si₂-type structure. A lot of the compounds have the AFM phase where the magnetic moments of Mn atoms are collinear in the xy plane. In the cases of $(X, Pn) = (\text{Ca}, \text{Sb})$ [S23], (Sr, As) [S24], and (Sr, Sb) [S25], the species is obtained as

$$\bar{3}m1' F2'/m, \quad (\text{S47})$$

which is full toroidic, and hence the AFM state is perfectly controllable by the electric current \mathbf{j} . With the site-symmetry group of Mn sites $\mathbf{H} = 3m$, the magnetic representation is given by

$$\Gamma_{\mathbf{G}}^{\text{mag}}(\mathbf{H}) = A_{2g} + E_g + B_{1u} + E_u. \quad (\text{S48})$$

The AFM state in the species (S47) is characterized by the E_u irreducible representation. This means that the AFM order is perfectly switchable by an in-plane electric current, since the basis of the E_u representation can be taken as the in-plane toroidal moment. Hence, the antiferromagnets belonging to the species (S47) may be a platform of the AFM spintronics. Thus, candidate materials are not restricted to the previously-studied tetragonal systems [S4, S19].

Most of the trigonal Mn 122-compounds are insulating or semiconducting. The switching may not be efficient, since the AFM Edelstein effect is determined by the Fermi-surface term [S6, S17]. On the other hand, it has been recently reported that EuMn_2As_2 becomes metallic by doping hole carriers [S26]. Although the magnetic structure of the doped system has not been identified, it may be a candidate for antiferromagnetic spintronics.

The trigonal XMn_2Pn_2 is a good example to illuminate a complementary role of two methods of symmetry analysis we present. In the case of $(X, \text{Pn}) = (\text{Ca}, \text{Bi})$ [S27], magnetic moments in the basal plane are slightly tilted from the basal rotation axes. The species is obtained as

$$\bar{3}m1' F\bar{1}'. \quad (\text{S49})$$

Therefore, the species of CaMn_2Bi_2 differs from that of other compounds (S47), while both magnetic structures are characterized by the E_u irreducible representation. Correspondingly, the domain states are different between the two species (S47) and (S49). Thus, although the magnetic representation characterizes the order parameter in the crystalline systems, stable domain states in the magnetic phase may not be uniquely determined. The domain states are completely elucidated with the use of the Aizu species analysis. The two symmetry analysis, the representation analysis and the Aizu species analysis, are complementary to each other.

TABLE S3: List of candidate materials for electrically switchable antiferromagnet. The table lists compounds, space group, symmetry of magnetic structure denoted by Aizu species and irreducible representations (Γ^{mag}), conducting properties (M/I), Néel temperatures (T_N), and references (Ref.). The blank part has not been clarified to the best of our knowledge. The numbers of the Aizu species and the space groups follow Ref. [S13] and [S28], respectively. All the compounds are characterized by the full toroidic species except for a partial toroidic compound $\text{U}_3\text{Ru}_4\text{Al}_{12}$. In the column of Γ^{mag} , the toroidal moments \mathbf{T} are also shown as the basis for the polar irreducible representations.

Compounds	Space group	Aizu species	Γ^{mag}	M/I	T_N	Ref.
CeMn_2Ge_2	$I4/mmm$ (139)	$4/mmm1' Fmmm' \langle x \rangle$ (218)	$E_u (\{T_x, T_y\})$		$318 < T < 417$	[S22]
CeMnAsO	$P4/nmm$ (129)	$4/mmm1' F4'/m'm'm$ (252)	B_{1u}		$35 < T < 340$	[S29]
		$4'/m'm'm Fm'mm' \langle x \rangle$ (-)	$E_u (\{T_x, T_y\})$		$7 < T < 35$	[S29]
		$m'mm' \langle x \rangle F2'/m \langle z \rangle$ (-)	$E_u (\{T_x, T_y\})$		7	[S29]
CeMnSbO	$P4/nmm$ (129)	$4/mmm1' F4'/m'm'm$ (252)	B_{1u}		$4.5 < T < 240$	[S30]
		$4'/m'm'm Fm'mm' \langle x \rangle$ (-)	$E_u (\{T_x, T_y\})$		4.5	[S30]
PrMnSbO	$P4/nmm$ (129)	$4/mmm1' F4'/m'm'm$ (252)	B_{1u}	metal	$35 < T < 230$	[S31]
		$4/mmm1' Fmmm' \langle x \rangle$ (218)	$E_u (\{T_x, T_y\})$	metal	35	[S31]
NdMnAsO	$P4/nmm$ (129)	$4/mmm1' F4'/m'm'm$ (252)	B_{1u}	semiconductor	$23 < T < 359$	[S32, S33]
		$4'/m'm'm Fmmm' \langle x \rangle$ (-)	$E_u (\{T_x, T_y\})$	semiconductor	23	[S32, S33]
DyB_4	$P4/mbm$ (127)	$4/mmm1' Fmmm' \langle x \rangle$ (218)	$E_u (\{T_x, T_y\})$	metal	$12.7 < T < 20.3$	[S34–S36]
ErB_4	$P4/mbm$ (127)	$4/mmm1' Fmmm' \langle x \rangle$ (218)	$E_u (\{T_x, T_y\})$	metal	13	[S34, S35, S37]
EuTiO_3	$I4_2/mcm$ (140)	$4/mmm1' Fmmm' \langle d \rangle$ (218)	$E_u (\{T_x, T_y\})$		5.3	[S38]
Mn_2Au	$I4/mmm$ (139)	$4/mmm1' Fmmm' \langle d \rangle$ (218)	$E_u (\{T_x, T_y\})$	metal	> 1000	[S39]
FeSn_2	$I4/mcm$ (140)	$4/mmm1' Fmmm' \langle d \rangle$ (218)	$E_u (\{T_x, T_y\})$	metal	$93 < T \lesssim 378$	[S40, S41]
		$mmm'(s) F2'/m \langle z \rangle$ (-)	$E_u (\{T_x, T_y\})$	metal	$93 \gtrsim T < 378$	[S40, S41]
CuMnAs	$P4/nmm$ (129)	$4/mmm1' Fmmm' \langle x \rangle$ (218)	$E_u (\{T_x, T_y\})$	semiconductor	480	[S3]
Cr_2WO_6	$P4_2/mnm$ (136)	$4/mmm1' Fmmm' \langle x \rangle$ (218)	$E_u (\{T_x, T_y\})$		45	[S42, S43]
Cr_2TeO_6	$P4_2/mnm$ (136)	$4/mmm1' Fmmm' \langle x \rangle$ (218)	$E_u (\{T_x, T_y\})$		93	[S42, S43]
$\text{U}_3\text{Ru}_4\text{Al}_{12}$	$P6_3/mmc$ (194)	$6/mmm1' Fmmm' \langle z \rangle$ (481)	$A_{2u}(T_z), E_{2u}$	metal	9.5	[S14, S44]

CaMn ₂ As ₂	P $\bar{3}m1$ (164)			semiconductor	62	[S45]
CaMn ₂ Sb ₂	P $\bar{3}m1$ (164)	$\bar{3}m1' F2'/m$ (295)	$E_u (\{T_x, T_y\})$	insulator	85	[S23]
		$\bar{3}m1' F\bar{1}'$ (286)	$A_{1u}, E_u (\{T_x, T_y\})$		85	[S46]
CaMn ₂ Bi ₂	P $\bar{3}m1$ (164)	$\bar{3}m1' F\bar{1}'$ (286)	$E_u (\{T_x, T_y\})$	semiconductor	154	[S27]
SrMn ₂ P ₂	P $\bar{3}m1$ (164)			semiconductor	53	[S47]
SrMn ₂ As ₂	P $\bar{3}m1$ (164)	$\bar{3}m1' F2'/m$ (295)	$E_u (\{T_x, T_y\})$	insulator	118	[S24, S45]
SrMn ₂ Sb ₂	P $\bar{3}m1$ (164)	$\bar{3}m1' F2'/m$ (295)	$E_u (\{T_x, T_y\})$	semiconductor	110	[S25]
EuMn ₂ As ₂	P $\bar{3}m1$ (164)			semiconductor	142	[S26]
YbMn ₂ Sb ₂	P $\bar{3}m1$ (164)	$\bar{3}m1' F1'$ (284)	$A_{1u}, E_u (\{T_x, T_y\})$		120	[S48]
Co ₄ Nb ₂ O ₉	P $\bar{3}c1$ (165)	$\bar{3}m1' F\bar{3}'m'$ (313)	A_{1u}	insulator	27.4	[S49]
		$\bar{3}m1' F2/m'$ (296)	$E_u (\{T_x, T_y\})$	insulator	27.2	[S50]
MnTiO ₃	R $\bar{3}$ (148)	$\bar{3}1' F\bar{3}'$ (264)	$A_u (T_z)$	insulator	64	[S51, S52]
MnGeO ₃	R $\bar{3}$ (148)	$\bar{3}1' F\bar{3}'$ (264)	$A_u (T_z)$		120	[S53]
NdCrTiO ₅	Pbam (55)	$mmm1' Fmmm'$ (71)	$B_{1u} (T_z)$	insulator	13	[S54]
					21	[S55]
LiFePO ₄	Pnma (62)	$mmm1' Fmmm'$ (71)	$B_{1u} (T_z)$	insulator	50	[S56]
		$mmm1' F2/m' \langle z \rangle$ (60)	$A_u, B_{1u} (T_z)$		47	[S57, S58]
LiNiPO ₄	Pnma (62)	$mmm1' Fmmm'$ (71)	$B_{2u} (T_y)$	insulator	20.8	[S59]
LiCoPO ₄	Pnma (62)	$mmm1' Fmmm'$ (71)	$B_{1u} (T_z)$	insulator	21.6	[S60, S61]
		$mmm1' F2' \langle x \rangle$ (53)	$B_{2g}, B_{1u} (T_z), B_{2u} (T_y)$			[S62, S63]
KMn ₄ (PO ₄) ₃	Pnam (62)	$mmm1' Fmmm'$ (73)	$B_{2u} (T_y)$		10	[S64]
t – NaFePO ₄	Pnma (62)	$mmm1' Fmmm'$ (71)	$B_{1u} (T_z)$		50	[S65]
Gd ₅ Ge ₄	Pnma (62)	$mmm1' Fmmm'$ (71)	$B_{1u} (T_z)$	metal	127	[S66, S67]
EuZrO ₃	Pnma (62)	$mmm1' Fmm'm$ (71)	$B_{2u} (T_y)$	insulator	4.1	[S68]
		$mmm1' Fm'm'm'$ (73)	A_u	insulator	4.4	[S69]
TbCoO ₃	Pbnm (62)	$mmm1' Fmmm'$ (71)	$B_{1u} (T_z)$	insulator	3.31	[S70]
HoCoO ₃	Pnma (62)	$mmm1' Fm'mm'$ (71)	$B_{2u} (T_y)$		3	[S71]
MnNb ₂ O ₆	Pbcn (60)	$mmm1' F2'/m \langle x \rangle$ (59)	$B_{2u} (T_y), B_{3u} (T_x)$		4.4	[S72]
CoSe ₂ O ₅	Pbcn (60)	$mmm1' Fm'mm$ (71)	$B_{3u} (T_x)$		8.5	[S73]
TbGe ₂	Cmmm (65)	$mmm1' Fm'mm$ (71)	$B_{3u} (T_x)$		41	[S74]
Ce ₃ Sn ₇	Cmmm (65)	$mmm1' Fm'mm$ (71)	$B_{3u} (T_x)$	metal	5	[S75, S76]
Sm ₃ Ag ₄ Sn ₄	Immm (71)	$mmm1' Fmmm'$ (71)	$B_{1u} (T_z)$		8.3	[S77]
		$mmm1' Fmm'm$ (71)	$B_{2u} (T_y)$		8.3	[S77]
UCu ₅ In	Pnma (62)	$mmm1' Fmm'm$ (71)	$B_{2u} (T_y)$	metal	25	[S78]
KFeO ₂	Pbca (61)	$mmm1' Fm'm'm'$ (73)	A_u		960	[S79]
		$mmm1' Fm'mm$ (71)	$B_{3u} (T_x)$		~ 1001	[S80]
CoGeO ₃	Pbca (61)	$mmm1' Fmmm'$ (71)	$B_{1u} (T_z)$	insulator	33.1	[S81]
DyVO ₄	Imma (74)	$mmm1' Fmmm'$ (71)	$B_{1u} (T_z)$	insulator	3.8	[S82, S83]
YbAl _{1-x} Fe _x B ₄	Pbam (55)	$mmm1' Fmmm'$ (71)	$B_{3u} (T_x)$	metal		[S84]
	Pbam (55)	$mmm1' Fm'm'm'$ (73)	A_u	metal		[S84]
Co ₃ TeO ₆	C2/c (15)	$2/m1' F2'/m$ (26)	$B_u (T_x, T_y)$		21.1	[S85]
MnPS ₃	C2/m (12)	$2/m1' F2'/m$ (26)	$B_u (T_x, T_y)$	insulator	78	[S86, S87]
LiFeSi ₂ O ₆	P2 ₁ /c (14)	$2/m1' F2/m'$ (27)	$A_u (T_z)$		17.8	[S88, S89]
		$2/m1' F\bar{1}'$ (17)	$A_u (T_z), B_u (T_x, T_y)$		18	[S90]
LiCrSi ₂ O ₆	P2 ₁ /c (14)	$2/m1' F2'/m$ (26)	$B_u (T_x, T_y)$		11.5	[S92]
LiCrGe ₂ O ₆	P2 ₁ /c (14)	$2/m1' F2'/m$ (26)	$B_u (T_x, T_y)$		4.8	[S91, S92]
LiVGe ₂ O ₆	P2 ₁ /c (14)		$A_u (T_z)$ or $B_u (T_x, T_y)$		24	[S93]
NaCrSi ₂ O ₆	C2/c (15)	$2/m1' F\bar{1}'$ (17)	$A_u (T_z), B_u (T_x, T_y)$		2.8	[S94]
CaMnGe ₂ O ₆	C2/c (15)	$2/m1' F\bar{1}'$ (17)	$A_u (T_z), B_u$		12	[S95]
		$2/m1' F2'/m$ (26)	$B_u (T_x, T_y)$	insulator	15	[S96]
MnGeO ₃	C2/c (15)	$2/m1' F2'/m$ (26)	$B_u (T_x, T_y)$		35.1	[S97]
Na ₂ RuO ₄	P2 ₁ /c (14)	$2/m1' F2/m'$ (27)	$A_u (T_z)$		37.22	[S98]

* watanabe.hikaru.43n@st.kyoto-u.ac.jp

- [S1] E. F. Bertaut, *Acta Crystallogr. Sect. A* **24**, 217 (1968).
- [S2] Y. A. Izyumov, R. Ozerov, and V. Naish, *Neutron diffraction of magnetic materials* (Springer, Berlin, 1991).
- [S3] P. Wadley, V. Novák, R. Campion, C. Rinaldi, X. Martí, H. Reichlová, J. Železný, J. Gazquez, M. Roldan, M. Varela, D. Khalyavin, S. Langridge, D. Kriegner, F. Máca, J. Mašek, R. Bertacco, V. Holý, A. Rushforth, K. Edmonds, B. Gallagher, C. Foxon, J. Wunderlich, and T. Jungwirth, *Nat. Commun.* **4**, 2322 (2013).
- [S4] P. Wadley, B. Howells, J. Elezny, C. Andrews, V. Hills, R. P. Campion, V. Novak, K. Olejnik, F. Maccherozzi, S. S. Dhesi, S. Y. Martin, T. Wagner, J. Wunderlich, F. Freimuth, Y. Mokrousov, J. Kune, J. S. Chauhan, M. J. Grzybowski, A. W. Rushforth, K. W. Edmonds, B. L. Gallagher, and T. Jungwirth, *Science* **351**, 587 (2016).
- [S5] T. Inui, Y. Tanabe, and Y. Onodera, *Group theory and its applications in physics*, Vol. Springer Series in Solid-State Sciences Vol. 78 (Springer, Berlin, 1990).
- [S6] J. Železný, H. Gao, A. Manchon, F. Freimuth, Y. Mokrousov, J. Zemen, J. Mašek, J. Sinova, and T. Jungwirth, *Phys. Rev. B* **95**, 014403 (2017).
- [S7] I. Garate and A. H. MacDonald, *Phys. Rev. B* **80**, 134403 (2009).
- [S8] C. Ciccarelli, L. Anderson, V. Tshitoyan, A. J. Ferguson, F. Gerhard, C. Gould, L. W. Molenkamp, J. Gayles, J. Železný, L. Šmejkal, Z. Yuan, J. Sinova, F. Freimuth, and T. Jungwirth, *Nat. Phys.* **12**, 855 (2016).
- [S9] H. Ohno, *Science* **281**, 951 (1998).
- [S10] A. Chernyshov, M. Overby, X. Liu, J. K. Furdyna, Y. Lyanda-Geller, and L. P. Rokhinson, *Nat. Phys.* **5**, 656 (2009).
- [S11] S. Esmailzadeh, U. Hålenius, and M. Valldor, *Chem. Mater.* **18**, 2713 (2006).
- [S12] V. Baltz, A. Manchon, M. Tsoi, T. Moriyama, T. Ono, and Y. Tserkovnyak, *Rev. Mod. Phys.* **90**, 015005 (2018).
- [S13] D. B. Litvin, *Acta Crystallogr. Sect. A Found. Crystallogr.* **64**, 316 (2008).
- [S14] R. Troć, M. Pasturel, O. Tougait, A. P. Sazonov, A. Gukasov, C. Sułkowski, and H. Noël, *Phys. Rev. B* **85**, 064412 (2012), although this paper mentioned that the magnetic order is identified as the $\Gamma_{12}(E_{2u})$ mode, the A_{2u} mode should be admixed to realize the magnetic structure in Fig. 3 of the paper.
- [S15] B. L. Chittari, Y. Park, D. Lee, M. Han, A. H. MacDonald, E. Hwang, and J. Jung, *Phys. Rev. B* **94**, 184428 (2016).
- [S16] C. Gong, L. Li, Z. Li, H. Ji, A. Stern, Y. Xia, T. Cao, W. Bao, C. Wang, Y. Wang, Z. Q. Qiu, R. J. Cava, S. G. Louie, J. Xia, and X. Zhang, *Nature (London)* **546**, 265 (2017).
- [S17] H. Watanabe and Y. Yanase, *Phys. Rev. B* **96**, 064432 (2017).
- [S18] H. Watanabe and Y. Yanase, *Phys. Rev. B* **98**, 245129 (2018).
- [S19] S. Y. Bodnar, L. Šmejkal, I. Turek, T. Jungwirth, O. Gomonay, J. Sinova, A. A. Sapozhnik, H.-J. Elmers, M. Kläui, and M. Jourdan, *Nat. Commun.* **9**, 348 (2018).
- [S20] Y. Singh, A. Ellern, and D. C. Johnston, *Phys. Rev. B* **79**, 094519 (2009).
- [S21] Y. Singh, M. A. Green, Q. Huang, A. Kreyssig, R. J. McQueeney, D. C. Johnston, and A. I. Goldman, *Phys. Rev. B* **80**, 100403 (2009).
- [S22] M. F. Md Din, J. L. Wang, Z. X. Cheng, S. X. Dou, S. J. Kennedy, M. Avdeev, and S. J. Campbell, *Sci. Rep.* **5**, 11288 (2015).
- [S23] D. E. McNally, J. W. Simonson, J. J. Kistner-Morris, G. J. Smith, J. E. Hassinger, L. DeBeer-Schmitt, A. I. Kolesnikov, I. A. Zaliznyak, and M. C. Aronson, *Phys. Rev. B* **91**, 180407 (2015).
- [S24] P. Das, N. S. Sangeetha, A. Pandey, Z. A. Benson, T. W. Heitmann, D. C. Johnston, A. I. Goldman, and A. Kreyssig, *J. Phys. Condens. Matter* **29**, 035802 (2017).
- [S25] N. S. Sangeetha, V. Smetana, A.-V. Mudring, and D. C. Johnston, *Phys. Rev. B* **97**, 014402 (2018).
- [S26] V. K. Anand and D. C. Johnston, *Phys. Rev. B* **94**, 014431 (2016).
- [S27] Q. D. Gibson, H. Wu, T. Liang, M. N. Ali, N. P. Ong, Q. Huang, and R. J. Cava, *Phys. Rev. B* **91**, 085128 (2015).
- [S28] M. I. Aroyo, *International Tables for Crystallography, Vol. A, Space-group symmetry* (International Union of Crystallography, 2016).
- [S29] Q. Zhang, W. Tian, S. G. Peterson, K. W. Dennis, and D. Vaknin, *Phys. Rev. B* **91**, 064418 (2015).
- [S30] Q. Zhang, C. M. N. Kumar, W. Tian, K. W. Dennis, A. I. Goldman, and D. Vaknin, *Phys. Rev. B* **93**, 094413 (2016).
- [S31] S. A. Kimber, A. H. Hill, Y.-Z. Zhang, H. O. Jeschke, R. Valentí, C. Ritter, I. Schellenberg, W. Hermes, R. Pöttgen, and D. N. Argyriou, *Physical Review B* **82**, 100412 (2010).
- [S32] A. Marcinkova, T. C. Hansen, C. Curfs, S. Margadonna, and J. W. G. Bos, *Phys. Rev. B* **82**, 174438 (2010).
- [S33] N. Emery, E. J. Wildman, J. M. S. Skakle, A. C. McLaughlin, R. I. Smith, and A. N. Fitch, *Phys. Rev. B* **83**, 144429 (2011).
- [S34] Z. Fisk, M. B. Maple, D. C. Johnston, and L. D. Woolf, *Solid State Commun.* **39**, 1189 (1981).
- [S35] G. Will and W. Schäfer, *J. Less-Common Met.* **67**, 31 (1979).
- [S36] S. Ji, C. Song, J. Koo, J. Park, Y. J. Park, K.-B. Lee, S. Lee, J.-G. Park, J. Y. Kim, B. K. Cho, K.-P. Hong, C.-H. Lee, and F. Iga, *Phys. Rev. Lett.* **99**, 076401 (2007).
- [S37] G. Will, W. Schäfer, F. Pfeiffer, F. Elf, and J. Etourneau, *J. Less-Common Met.* **82**, 349 (1981).
- [S38] V. Scagnoli, M. Allieta, H. Walker, M. Scavini, T. Katsufuji, L. Sagarna, O. Zaharko, and C. Mazzoli, *Phys. Rev. B* **86**, 094432 (2012).
- [S39] V. M. T. S. Barthem, C. V. Colin, H. Mayaffre, M.-H. Julien, and D. Givord, *Nat. Commun.* **4**, 2892 (2013).
- [S40] G. Venturini, B. Malaman, G. Le Caër, and D. Fruchart, *Phys. Rev. B* **35**, 7038 (1987).

- [S41] M. Armbrüster, W. Schnelle, R. Cardoso-Gil, and Y. Grin, *Chem. - A Eur. J.* **16**, 10357 (2010).
- [S42] W. Kunmann, S. L. Placa, L. Corliss, J. Hastings, and E. Banks, *Journal of Physics and Chemistry of Solids* **29**, 1359 (1968).
- [S43] M. Zhu, D. Do, C. R. Dela Cruz, Z. Dun, H. D. Zhou, S. D. Mahanti, and X. Ke, *Phys. Rev. Lett.* **113**, 076406 (2014).
- [S44] M. Pasturel, O. Tougait, M. Potel, T. Roisnel, K. Wochowski, H. Noël, and R. Troć, *J. Phys. Condens. Matter* **21**, 125401 (2009).
- [S45] N. S. Sangeetha, A. Pandey, Z. A. Benson, and D. C. Johnston, *Phys. Rev. B* **94**, 094417 (2016).
- [S46] C. A. Bridges, V. V. Krishnamurthy, S. Poulton, M. P. Paranthaman, B. C. Sales, C. Myers, and S. Bobev, *J. Magn. Magn. Mater.* **321**, 3653 (2009).
- [S47] S. L. Brock, J. Greedan, and S. M. Kauzlarich, *J. Solid State Chem.* **113**, 303 (1994).
- [S48] A. V. Morozkin, O. Isnard, P. Henry, S. Granovsky, R. Nirmala, and P. Manfrinetti, *J. Alloys Compd.* **420**, 34 (2006).
- [S49] E. Bertaut, L. Corliss, F. Forrat, R. Aleonard, and R. Pauthenet, *J. Phys. Chem. Solids* **21**, 234 (1961).
- [S50] N. D. Khanh, N. Abe, H. Sagayama, A. Nakao, T. Hanashima, R. Kiyonagi, Y. Tokunaga, and T. Arima, *Phys. Rev. B* **93**, 075117 (2016).
- [S51] H. J. Silverstein, E. Skoropata, P. M. Sarte, C. Mauws, A. A. Aczel, E. S. Choi, J. van Lierop, C. R. Wiebe, and H. Zhou, *Phys. Rev. B* **93**, 054416 (2016).
- [S52] G. Shirane, S. J. Pickart, and Y. Ishikawa, *J. Phys. Soc. Jpn.* **14**, 1352 (1959).
- [S53] K. Tsuzuki, Y. Ishikawa, N. Watanabe, and S. Akimoto, *J. Phys. Soc. Jpn.* **37**, 1242 (1974).
- [S54] G. Buisson, *J. Phys. Chem. Solids* **31**, 1171 (1970).
- [S55] J. Hwang, E. S. Choi, H. D. Zhou, J. Lu, and P. Schlottmann, *Phys. Rev. B* **85**, 024415 (2012).
- [S56] R. P. Santoro and R. E. Newnham, *Acta Crystallogr.* **22**, 344 (1967).
- [S57] J. Li, V. O. Garlea, J. L. Zarestky, and D. Vaknin, *Phys. Rev. B* **73**, 024410 (2006).
- [S58] R. Toft-Petersen, M. Reehuis, T. B. S. Jensen, N. H. Andersen, J. Li, M. D. Le, M. Laver, C. Niedermayer, B. Klemke, K. Lefmann, and D. Vaknin, *Phys. Rev. B* **92**, 024404 (2015).
- [S59] I. Kornev, M. Bichurin, J.-P. Rivera, S. Gentil, H. Schmid, A. G. M. Jansen, and P. Wyder, *Phys. Rev. B* **62**, 12247 (2000).
- [S60] E. Fogh, R. Toft-Petersen, E. Ressouche, C. Niedermayer, S. L. Holm, M. Bartkowiak, O. Prokhnenko, S. Sloth, F. W. Isaksen, D. Vaknin, and N. B. Christensen, *Phys. Rev. B* **96**, 104420 (2017).
- [S61] R. Santoro, D. Segal, and R. Newnham, *Journal of Physics and Chemistry of Solids* **27**, 1192 (1966).
- [S62] D. Vaknin, J. L. Zarestky, L. L. Miller, J.-P. Rivera, and H. Schmid, *Phys. Rev. B* **65**, 224414 (2002).
- [S63] B. B. Van Aken, J.-P. Rivera, H. Schmid, and M. Fiebig, *Nature (London)* **449**, 702 (2007).
- [S64] M. L. López, A. Daidouh, C. Pico, J. Rodríguez-Carvajal, and M. L. Veiga, *Chem. - A Eur. J.* **14**, 10829 (2008).
- [S65] M. Avdeev, Z. Mohamed, C. D. Ling, J. Lu, M. Tamaru, A. Yamada, and P. Barpanda, *Inorg. Chem.* **52**, 8685 (2013).
- [S66] L. Tan, A. Kreyssig, J. W. Kim, A. I. Goldman, R. J. McQueeney, D. Wermeille, B. Sieve, T. A. Lograsso, D. L. Schlagel, S. L. Budko, V. K. Pecharsky, and K. A. Gschneidner, *Phys. Rev. B* **71**, 214408 (2005).
- [S67] E. M. Levin, V. K. Pecharsky, K. A. Gschneidner, and G. J. Miller, *Phys. Rev. B* **64**, 235103 (2001).
- [S68] M. Avdeev, B. J. Kennedy, and T. Kolodiazny, *J. Phys. Condens. Matter* **26**, 095401 (2014).
- [S69] R. Saha, A. Sundaresan, M. K. Sanyal, C. N. R. Rao, F. Orlandi, P. Manuel, and S. Langridge, *Phys. Rev. B* **93**, 014409 (2016).
- [S70] K. Knížek, Z. Jiráček, P. Novák, and C. de la Cruz, *Solid State Sci.* **28**, 26 (2014).
- [S71] A. Muñoz, M. J. Martínez-Lope, J. A. Alonso, and M. T. Fernández-Díaz, *Eur. J. Inorg. Chem.* **76**, 5825 (2012).
- [S72] O. V. Nielsen, B. Lebech, F. K. Larsen, L. M. Holmes, and A. A. Ballman, *J. Phys. C Solid State Phys.* **9**, 2401 (1976).
- [S73] B. C. Melot, B. Paden, R. Seshadri, E. Suard, G. Nénert, A. Dixit, and G. Lawes, *Phys. Rev. B* **82**, 014411 (2010).
- [S74] P. Schobinger-Papamantellos, D. De Mooij, and K. Buschow, *J. Less Common Met.* **144**, 265 (1988).
- [S75] M. Bonnet, J. X. Boucherle, F. Givord, F. Lapierre, P. Lejay, J. Odin, A. P. Murani, J. Schweizer, and A. Stunault, *J. Magn. Magn. Mater.* **132**, 289 (1994).
- [S76] F. Givord, P. Lejay, E. Ressouche, J. Schweizer, and A. Stunault, *Phys. B Condens. Matter* **156-157**, 805 (1989).
- [S77] C. J. Voyer, D. H. Ryan, J. M. Cadogan, L. M. D. Cranswick, M. Napoletano, P. Riani, and F. Canepa, *J. Phys. Condens. Matter* **19**, 436205 (2007).
- [S78] V. H. Tran, D. Kaczorowski, R. Troć, G. André, F. Bourée, and V. Zaremba, *Solid State Commun.* **117**, 527 (2001).
- [S79] Z. Tomkowicz and A. Szytuea, *J. Phys. Chem. Solids* **38**, 1117 (1977).
- [S80] D. Sheptyakov, N. Z. Ali, and M. Jansen, *J. Phys. Condens. Matter* **22**, 426001 (2010).
- [S81] G. J. Redhammer, A. Senyshyn, G. Tippelt, C. Pietzonka, G. Roth, and G. Amthauer, *Phys. Chem. Miner.* **37**, 311 (2010).
- [S82] G. Will and W. Schafer, *J. Phys. C Solid State Phys.* **4**, 811 (1971).
- [S83] K. Kishimoto, T. Ishikura, H. Nakamura, Y. Wakabayashi, and T. Kimura, *Phys. Rev. B* **82**, 012103 (2010).
- [S84] S. Suzuki and S. Nakatsuji, private communication.
- [S85] S. Ivanov, R. Tellgren, C. Ritter, P. Nordblad, R. Mathieu, G. André, N. Golubko, E. Politova, and M. Weil, *Mater. Res. Bull.* **47**, 63 (2012).
- [S86] K. Kurosawa, S. Saito, and Y. Yamaguchi, *J. Phys. Soc. Jpn.* **52**, 3919 (1983).
- [S87] E. Ressouche, M. Loire, V. Simonet, R. Ballou, A. Stunault, and A. Wildes, *Phys. Rev. B* **82**, 100408 (2010).
- [S88] G. J. Redhammer, G. Roth, W. Treutmann, M. Hoelzel, W. Paulus, G. André, C. Pietzonka, and G. Amthauer, *J. Solid State Chem.* **182**, 2374 (2009).
- [S89] G. J. Redhammer, G. Roth, W. Paulus, G. André, W. Lottermoser, G. Amthauer, W. Treutmann, and B. Koppelhuber-

- Bitschnau, *Phys. Chem. Miner.* **28**, 337 (2001).
- [S90] P. Tolédano, M. Ackermann, L. Bohatý, P. Becker, T. Lorenz, N. Leo, and M. Fiebig, *Phys. Rev. B* **92**, 094431 (2015).
- [S91] G. Nénert, M. Isobe, C. Ritter, O. Isnard, A. N. Vasiliev, and Y. Ueda, *Phys. Rev. B* **79**, 064416 (2009).
- [S92] G. Nénert, M. Isobe, I. Kim, C. Ritter, C. V. Colin, A. N. Vasiliev, K. H. Kim, and Y. Ueda, *Phys. Rev. B* **82**, 024429 (2010).
- [S93] M. D. Lumsden, G. E. Granroth, D. Mandrus, S. E. Nagler, J. R. Thompson, J. P. Castellán, and B. D. Gaulin, *Phys. Rev. B* **62**, R9244 (2000).
- [S94] G. Nénert, I. Kim, M. Isobe, C. Ritter, A. N. Vasiliev, K. H. Kim, and Y. Ueda, *Phys. Rev. B* **81**, 184408 (2010).
- [S95] G. J. Redhammer, G. Roth, W. Treutmann, W. Paulus, G. André, C. Pietzonka, and G. Amthauer, *J. Solid State Chem.* **181**, 3163 (2008).
- [S96] L. Ding, C. V. Colin, C. Darie, J. Robert, F. Gay, and P. Bordet, *Phys. Rev. B* **93**, 064423 (2016).
- [S97] G. J. Redhammer, A. Senyshyn, G. Tippelt, and G. Roth, *J. Phys. Condens. Matter* **23**, 254202 (2011).
- [S98] K. M. Mogare, D. V. Sheptyakov, R. Bircher, H.-U. Güdel, and M. Jansen, *Eur. Phys. J. B* **52**, 371 (2006).